Doctoral Thesis

Pib2 is a cysteine sensor involved in TORC1 activation in *Saccharomyces cerevisiae*

Qingzhong Zeng

August 2023

Center for Frontier Oral Science

Graduate School of Frontier Biosciences

Osaka University

Abstract

TORC1 is a master regulator that integrates information from multiple upstream signals and phosphorylates substrates to promote anabolism and cell growth, upon amino acids were sufficient. In the absence of amino acids, TORC1 is inactive and autophagy is induced to degrade intracellular proteins for recycling amino acids. It is activated via two distinct upstream pathways, the Gtr pathway, which corresponds to mammalian Rag, and the Pib2 pathway. In mammals, it has been reported that several amino acid sensors regulate GATOR2-GATOR1-Rag GTPase axis to trigger TORC1 activity. However, how amino acids are sensed is poorly understood in *Saccharomyces cerevisiae*. Sch9, one of the TORC1 substrates, is phosphorylated via the Pib2 pathway and the Gtr pathway. Ser3, a novel TORC1 substrate, is phosphorylated by the Pib2 pathway and not by the Gtr pathway. In this study, using the phosphorylation state of Sch9 and Ser3 as indicators of TORC1 activity, I investigated which pathways were employed in TORC1 activation by individual amino acid. Different amino acids exhibited different dependencies on the Gtr and Pib2 pathways.

Cysteine was the amino acid most dependent on the Pib2 pathway. Cysteine induces a dose-dependent increase in the interaction between TOR1 and Pib2 *in vivo* and *in vitro*. Moreover, cysteine directly bound to Pib2 via W632 and F635, two critical residues in the T(ail) motif that are necessary to activate TORC1. These results indicate that Pib2 functioning as a sensor for cysteine in TORC1 regulation.

Contents

1. General introduction

1.1 History of TOR research

The research of TOR commenced with the discovery of rapamycin. In 1965, rapamycin was isolated from a soil sample collected on Easter Island. It is a secondary metabolite secreted from actinomyces, *Streptomyces hygroscopicus*. This compound is named after the native name of the island, Rapa Nui. The research of rapamycin was initially focused on its antifungal capacity against *Candida albicans*[1]. Subsequently, it was recognized for its effectiveness as an immunosuppressant and an anti-tumor agent, and has been employed to prevent immune rejection of organ transplantation and treat tumor, respectively[2,3]. FK506 is another immunosuppressive medication with similar characteristics and chemical structure comparable to rapamycin. In 1990, Stuart Schreiber found that FK506 and rapamycin bind to the same site on FK506-binding protein 12 (FKBP12), and proposed a model in which these compounds have activity when they interact with FKBP12, then interact with distinct proteins[4,5]. In 1991, Michael Hall successfully identified rapamycin-resistant mutants in *S. cerevisiae* using a genetic screen that included *FPR1*, a FK506-sensitive proline rotamase, and two unknown function genes[6]. *FPR1* is a yeast orthologue of FKBP12, and two unreported genes encode Ser/Thr protein kinase with 67% identity, *TOR1* and *TOR2*, which are the mechanistic targets of rapamycin[6]. In 1994-1995, David Sabatini and his colleagues demonstrated that mTOR

(mammalian TOR) is FKBP12-rapamycin interacting protein in mammals[7–9]. In 1997, Takeshi Noda and Yoshinori Oshumi investigated that TOR suppressed autophagy in *S. cerevisiae*[10]. Since these discoveries, TOR has been extensively studied, leading to a further understanding of its mechanisms, and it has become a prominent topic of research in the scientific community.

1.2 The components of TORC1 and TORC2

In the early years of TOR research, genetic evidences suggested the existence of two distinct TOR signaling pathways in yeast and mammals, the rapamycin-sensitive pathway and the rapamycin-insensitive pathway. The TOR pathway that is sensitive to rapamycin is known as TOR Complex 1 (TORC1 and mTORC1), while the rapamycin-insensitive pathway is called TOR Complex 2 (TORC2 and mTORC2)[11–13]. In mammals, mTORC1 consists of mTOR, Raptor, mLST8, PRAS40 and DEPTOR[14–18], and mTORC2 consists of mTOR, Rictor, mLST8, mSin1, Protor and DEPTOR (Figure IA, IB) [11,13,17,19–22]. In yeast, TORC1 is composed of Tor1 or Tor2, Kog1, Lst8 and Tco89[12,23,24], and TORC2 is composed of Tor2, Avo1, Avo2, Avo3 and Lst8 (Figure IC, ID)[12,23–25]. Despite the fact that TOR1 and TOR2 are quite homologous, individual deletion mutants exhibit distinct phenotypes. TORC1 is inhibited by binding FKBP-rapamycin and regulates cellular processes such as growth, metabolism, and aging in response to nutrient availability and other environmental stress[26]. TORC2 is less well understand but involved

in controlling processes such as cell polarity, actin cytoskeleton dynamics, and cell survival[26].

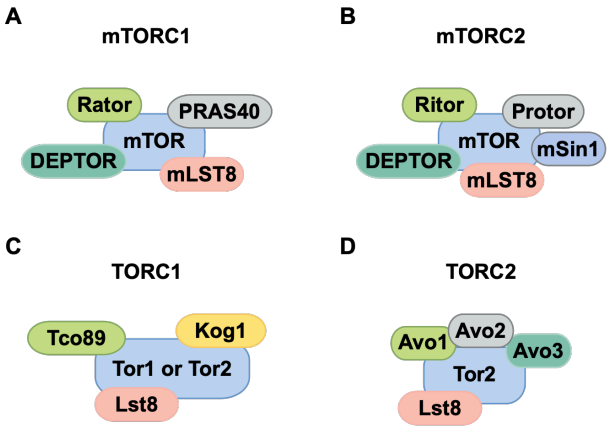

Figure I**. Composition of mTORC1, mTORC2, TORC1 and TORC2**
(A) mTORC1 subunits: mTOR, Raptor, mLST8, PRAS40 and DEPTOR. **(B)** mTORC2 subunits: mTOR, Rictor, mLST8, Sin1, Protor and DEPTOR. **(C)** TORC1 subunits: Tor1 or Tor2, Kog1, Lst8 and Tco89. **(D)** TORC2 subunits: Tor2, Avo1, Avo2, Avo3 and Lst8.

1.3 Downstream of TORC1 pathway

Upon nutrition addition, it stimulates cell growth by upregulating the synthesis of proteins, nucleotides, and lipids while simultaneously suppressing catabolic processes like autophagy. Conversely, when nutrient availability is restricted, cells suppress anabolic processes and boost catabolic processes such as autophagy to maintain cell survival. TORC1 serves as a pivotal mediator in coordinating these cellular processes, therefore enabling the maintenance of homeostasis between anabolism and catabolism in response to diverse environment conditions. Yeast Sch9 is mammalian ortholog S6 Kinase 1 (S6K1), which belong to the AGC family kinase. It is a substrate of TORC1 and localizes on the vacuole membrane. TORC1 phosphorylates the T737 residue of Sch9,

which is found in a classical hydrophobic motif (Figure II)[27]. TORC1 regulates protein synthesis, cell growth, and aging by phosphorylating Sch9[26]. Atg13 (autophagy-related protein 13) is also a substrate of TORC1, which is crucial in autophagy and is phosphorylated on S554 site by TORC1 (Figure II)[10]. When TORC1 is inactivated, dephosphorylated Atg13 interacts with Atg1 and Atg17, triggering the formation of pre-autophagosomal structures (PAS). When nutrition is abundant, TORC1 phosphorylates Atg13, preventing it from forming pre-autophagosomal structures, thereby inhibiting autophagy[28]. Other substrates directly phosphorylated by TORC1 include Sfp1[29], Gln3[30], Sit4[31], and Ypk3[32] (Figure II), which are involved in the coordination of cellular processes in response to environmental stresses.

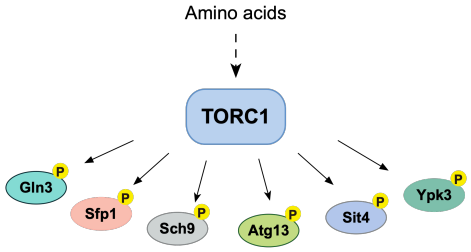

Figure II**. Substrates of TORC1**
Gln3, Sfp1, Sch9, Atg13, Sit4 and Ypk3 are phosphorylated by activated TORC1.

1.4 Upstream pathway of TORC1

One of the extensively studied aspects of TORC1 is its upstream regulatory mechanism, which contributes to understand how TORC1 smoothly and strictly integrates multiple inputs to coordinate cell growth and metabolism. Numerous studies have indicated that various inputs such as amino acids, glucose, insulin and hypoxia

regulate the TORC1 pathway, however the molecular mechanisms by which these inputs regulate TORC1 remain to be explored. In mammals, insulin stimulate Akt (also known as Protein kinase B), and directly phosphorylates Tuberous sclerosis complex 2 (TSC2). Tuberous sclerosis complex 1/2 (TSC1/2) is GTPase activating protein (GAP) of small GTP-binding protein, the Ras homology enriched in brain (Rheb). Phosphorylated TSC1/2 negatively regulate Rheb[33–35]. Rheb is localized on lysosomes and/or Golgi, and active GTP-bound form Rheb activate TORC1 by direct interaction[36]. Ragulator complex (p18, p14, MP1, C7ORF59, HBXIP, LAMTOR1-5) recruits Rag GTPase (heterodimeric of RagA/B and Rag C/D) to the lysosome membrane[37,38]. Amino acids activate the Rag GTPase, and then activated Rag complex recruit mTORC1 from the cytoplasm to lysosomes, where it encounters with the small GTPase Rheb and leads to mTORC1 activation (Figure I-3)[38–41]. The heterodimeric small GTPases, Gtr1-Gtr2 (the Gtr complex) are the yeast homolog of RagA/B-RagC/D (the Rag complex). Gtr complex is anchored to the vacuolar membranes via the EGO complex, which consists of Ego1, Ego2 and Ego3, possessing similar architecture with Ragulator and activate TORC1[42,43]. GATOR1 (Nprl2, Nprl3 and DEPDC5) and GATOR2 (WDR24, WDR59, Mios, Seh1l and Sec13) are identified by mass spectrometric analysis, which regulate Rag GTPase pathway[44]. GATOR1 suppresses mTORC1 via acting as a GTPase-activating protein (GAP) for RagA/B, while GATOR2 activates mTORC1 by inhibiting GATOR1 (Figure III)[44,45]. Subsequently, in budding yeast, SEACIT (Npr2, Npr3 and Iml1) and SEACAT (Seh1, Sea2, Sea3, Sea4 and Sec13) were identified as homologues of GATOR1 and

GATOR2 respectively, and them regulate the Gtr pathway[46,47]. Meanwhile, SEACIT suppresses TORC1 by functioning as a GTPase-activating protein (GAP) for Gtr1, whereas SEACAT suppresses TORC1 by inhibiting SEACIT (Figure III)[48–50]. Therefore, Gtr GTPase, an upstream regulator of TORC1, is highly conserved from yeast to mammals. Recently, Pib2, another upstream of TORC1, has also been identified in yeast (Figure III)[51–54]. These studies suggest that TORC1 is activated by two parallel upstream pathways, the Gtr pathway and the Pib2 pathway.

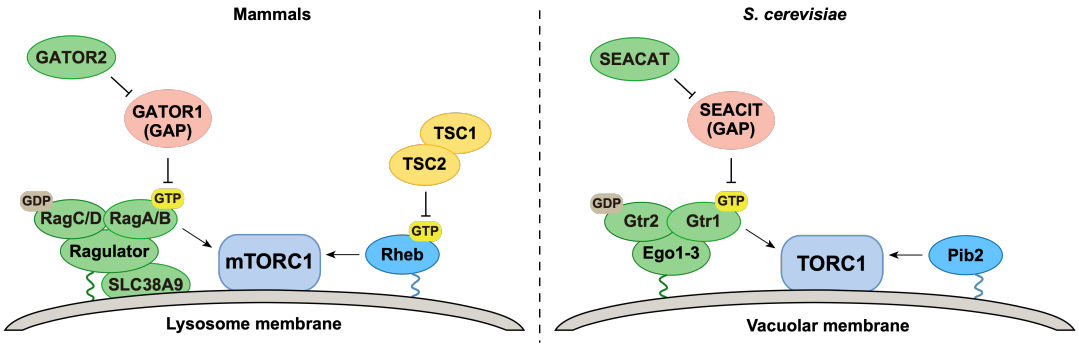

Figure III**. Upstream of mTORC1 in mammals and TORC1 in yeast**
The GATOR2-GATOR1-Rag GTPase and TSC-Rheb pathways are upstream of mTORC1 (left). The Gtr and Pib2 pathways are upstream of TORC1 (right). GAP in parentheses signifies that the protein acts as an activator of GTPase.

1.5 Amino acids regulates TORC1

TORC1 integrates nutrient signals and phosphorylates substrates to regulate cell growth and metabolism. Amino acids are particularly important TORC1 activators in budding yeast. However, the mechanism by which amino acids regulate TORC1 remained elusive until the breakthrough discovery that amino acids regulate mTORC1

via the heterodimeric Rag GTPase[39,40]. After that, it has been reported that GATOR1 and GATOR2 complexes are involved in sensing and transmitting signals form specific amino acids to mTORC1. In response to particular amino acids, such as leucine and arginine, GATOR2 stimulates mTORC1 activation and counteracts the inhibitory impact of GATOR1[44]. Sestrin2 interacts with GATOR2 to inhibit mTORC1 when amino acids decrease, revealing important insight on the mechanism of amino acid sensing[55,56]. Sestrin2 is a leucine sensor that binds to GATOR2 to block its function in the deficiency of leucine and dissociates from it upon leucine binding (Figure IV)[57,58]. In a manner similar to Sestrin2, CASTOR1 is an arginine sensor that binds to GATOR2 to inhibit its activity in the deficiency of arginine, and dissociates from it upon arginine binding (Figure IV)[59,60]. SAMTOR is a S-adenosylmethionine (SAM) sensor that binds and inhibits GATOR1 in the absence of methionine, converts methionine to SAM when methionine is present and dissociates SAMTOR from GATOR1 upon binding to SAM (Figure IV)[61]. SAR1B is another leucine sensor which, similar to Sestrin2, binds to GATOR2 to block its function in the absence of leucine and dissociates from it when leucine is bound (Figure IV)[62]. The amino acid sensors discovered here help us better understand how mammalian cells react to amino acid availability, but they are not conserved in budding yeast. It is possible that the absence of conservation of certain mammalian amino acid sensors in yeast is due to the difference in nutritional requirements. Mammals are heterotrophic, relying on external sources for amino acids, while yeast is autotrophic and can synthesize its own amino acids. There are reports suggesting that

leucine and methionine activate TORC1 via the Gtr pathway (Figure IV)[42,63,64]. Recently, Glutamine was found to activate TORC1 mainly through the Pib2 pathway and to activate TORC1 in the presence of Pib2 in vitro (Figure IV)[53,54,65]. Whether Pib2 directly binds to glutamine and acts as a direct glutamine sensor remains unknown. The study of the mechanism underlying amino acid sensing by TORC1 is interesting and urgently needed to help understand how cells rapidly detect changes in nutrition levels and thus coordinate cell growth and metabolism.

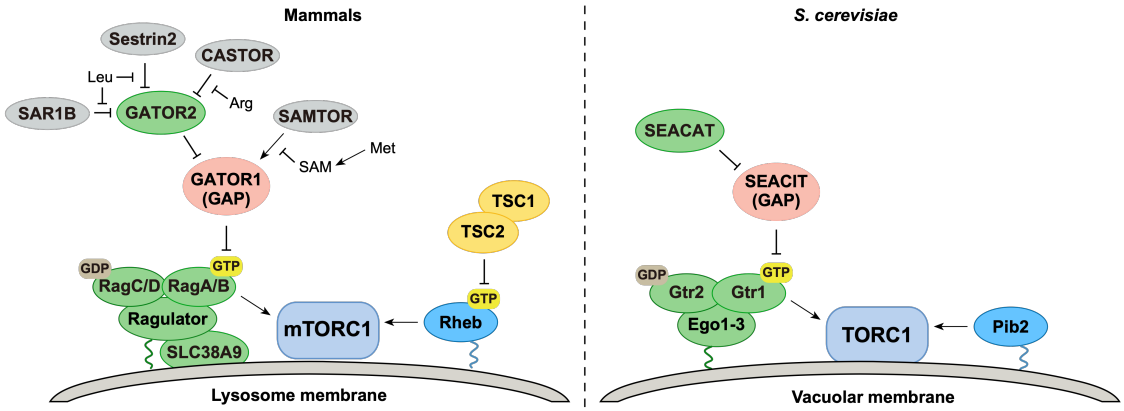

Figure IV**. Amino acid sensing pathway of mTORC1 and TORC1**
Proteins shown in gray are specific amino acid sensors. Amino acid sensing pathways upstream of mammalian mTORC1 (left) and yeast TORC1 (right).

1.6 Introduction of this thesis

Living organisms must be capable of sensing internal and external environmental changes promptly and efficiently, and to respond appropriately to these changes to maintain homeostasis. They achieve this through signaling cascades that rapidly and rigorously integrate numerous environmental inputs and transmit this

information to metabolic regulators to control anabolic and catabolic processes. Target of rapamycin complex 1 (TORC1) or mechanistic target of rapamycin complex 1 (mTORC1) is a master regulator of cell growth that is highly conserved across eukaryotes, and it responds to nutrient levels to coordinate metabolism and cell growth[26,66].

In the budding yeast *S. cerevisiae*, TORC1 is comprised of a central protein kinase[26]. When amino acids are available, TORC1 promotes anabolic processes such as protein synthesis by phosphorylating Sch9, the homologue of S6 kinase (S6K) in mammals[27,67]. At the same time, TORC1 suppresses catabolic processes such as autophagy by phosphorylating the autophagy-related protein Atg13[10,68]. These effects are reversed during conditions of amino acid or nitrogen starvation; upon nitrogen starvation, Atg13 is dephosphorylated and enhances the formation of protein condensates termed the PAS, which is comprised of most autophagy related proteins including Atg2[68–71].

TORC1 activity is regulated by the GATOR2-GATOR1-Rag GTPase axis in mammals, and the SEACAT-SEACIT-Gtr GTPase axis in yeast[40,42]. Under amino acid-rich conditions, GATOR1 is suppressed by GATOR2, its negative regulator[44]. Meanwhile, RagA/B takes GTP form to recruit mTORC1 to lysosomes, where Rheb encounters with mTORC1 resulting in its activation[41]. Under amino acid deficiency, GATOR2 dissociates from and activates GATOR1[44,45]. Activated GATOR1 promotes RagA/B to takes the GTP-bound form, resulting in the inactivation of mTORC1[44]. Inactivated mTORC1

dissociates from lysosomes to cytoplasm. Similar to mammals, in budding yeast, SEACIT is inhibited by SEACAT, when amino acids are abundant. Moreover, Gtr1 take GTP form to activate TORC1 on the vacuolar membrane. When amino acids are deficient, SEACAT dissociates from and activates SEACIT. Activated SEACIT induces Gtr1 to takes the GTP-bound form, resulting in the inactivation of TORC1[47–50]. Different from dissociation from lysosomes in mammals, inactivated TORC1 becomes puncta associating with the vacuole, and activated TORC1 disperses on the vesicle membrane[47,72]. It is still uncertain whether a functional counterpart of Rheb exists in budding yeast.

Recently, there has emerged a class of proteins that function as amino acid sensors in mammals. Sestrin2 was the first leucine sensor to be identified. When leucine is abundant, Sestrin2 binds to leucine and becomes unable to bind to GATOR2, which enables GATOR2 to function as a GATOR1 inhibitor, leading to mTORC1 activation[73]. Several other amino acid sensors have been reported: CASTOR, an arginine sensor, SAMTOR, a methionine (SAM) sensor, and SAR1B, another leucine sensor[59,61,62]. Although these findings have advanced my understanding of how mammalian cells respond to amino acid availability, these amino acid sensors are not conserved in the budding yeast.

Pib2 was recently characterized as a TORC1 regulator that functions outside of the Gtr pathway in *S. cerevisiae*[52–54,74]. It also associates with the vacuolar membrane by its FYVE domain, which interacts with phosphatidylinositol 3-phosphate (PtdIns3P)[52–

[54,74]. Cells deficient in Gtr1 or Pib2 alone are still able to grow, but their double knockout leads to synthetic lethality[52,74]. Conditional mutation in Gtr1 and Pib2 resulted in the loss of TOC1 activity[54]. These above studies indicate that TORC1 activation occurs through two parallel upstream pathways, the Gtr pathway and the Pib2 pathway. Interestingly, Pib2 serve as a main component of the glutamine sensor, and glutamine facilitates Pib2-TORC1 interaction to activate TORC1[54,65]. Despite these reports, the molecular mechanisms by which individual amino acid activates TORC1 remain largely unclear, especially in budding yeast.

There are at least two separate phases whereby amino acids activate TORC1 after nitrogen starvation; phase 1 involves acute, transient activation at around 5 min, and phase 2 is characterized by slow, continuous activation later than 15 min[38,75]. In, phase 2, prototrophic yeast is able to convert any amino acid to any other amino acids through metabolic reactions. Auxotrophy in the parental strain can result in potential bias when analyzing physiological quantitative parameters in metabolic networks. By contrast, in phase 1, TORC1 may react to individual amino acid species before they are metabolized. Therefore, I studied brief amino acid stimulation to investigate how TORC1 monitors individual amino acids.

Using the well-established TORC1 substrate Sch9 and the novel TORC1 substrate Ser3, the latter of which is specifically phosphorylated by the Pib2 pathway, I analyzed the relationships between 20 amino acids and the Gtr and Pib2 pathways. I

discovered that cysteine activates TORC1 in a manner dependent on the Pib2 pathway, and enhances Pib2-TORC1 interaction by directly binding to Pib2. Thus, Pib2 serves as a cysteine sensor in the TORC1 pathway.

2. Results

2.1 Different upstream signals of TORC1 regulate distinct TORC1 substrates

In order to investigate the potential differential sensing of amino acids by the two upstream pathways of TORC1, the Gtr and Pib2 pathways, I monitored the status of TORC1 activity by following phosphorylation of two independent TORC1 substrates: One is well established Sch9[27] and another is Ser3, which was recently identified as a novel TORC1 substrate by Dr. Araki.

Here, in wild-type cells, Sch9 was phosphorylated under nutrient-rich growing conditions, as detected by phosphor-specific Sch9 (T737) antibody (Figure 1A)[27,76]. This phosphorylation was suppressed by treatment with rapamycin, a TORC1 inhibitor, and enhanced by cycloheximide, a TORC1 activator (Figure 1A)[6,42]. Although simultaneous abrogation of the Gtr and Pib2 pathways led to complete abolition of Sch9 phosphorylation[54], this phosphorylation was only slightly suppressed by *gtr1*Δ or *pib2*Δ cells individually (Figure 1A), indicating that TORC1 can phosphorylate Sch9 via either the Gtr pathway or the Pib2 pathway. The upshifted phosphorylated band of Ser3-3HA was suppressed by rapamycin treatment and enhanced by cycloheximide treatment (Figure 1A), indicating that Ser3 is a bona fide TORC1 substrate. Ser3 phosphorylation was observed in untreated *gtr1*Δ cells and was further enhanced by cycloheximide

treatment (Figure 1A). In sharp contrast, Ser3 phosphorylation was totally suppressed during growth conditions in *pib2*Δ cells, and even after cycloheximide treatment, which suggested that Ser3 is a specific substrate of Pib2 dependent pathway (Figure 1A). These results suggest that Sch9 phosphorylation is regulated by either the Gtr pathway or the Pib2 pathway, whereas Ser3 phosphorylation is mainly dependent on the Pib2 pathway (Figure 1B).

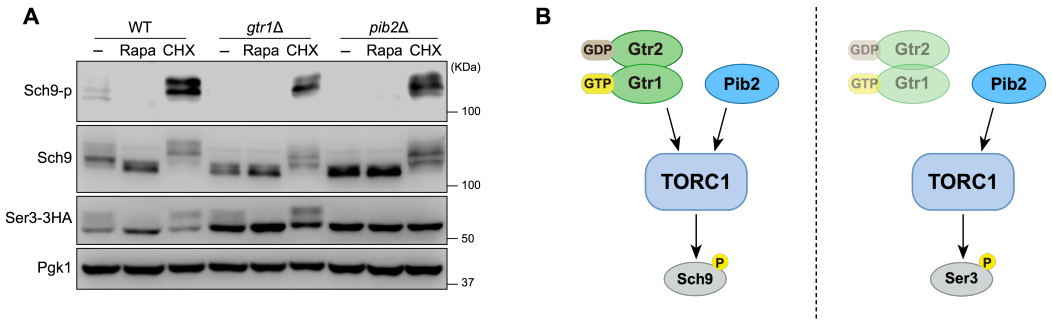

Figure 1. Different upstream inputs of TORC1 exhibit distinct regulatory effects on TORC1 substrates

(A) Wild-type (YAY2864), *gtr1*Δ (YAY2867), and *pib2*Δ (YAY2868) cells grown in YPD medium were treated with 0.2 μg/mL rapamycin (Rapa) or 25 μg/mL cycloheximide (CHX) for 30 min. Cell lysates were analyzed by western blotting using anti-Sch9-p (T737), anti-Sch9, anti-HA, anti-Pgk1 antibodies. **(B)** Sch9 phosphorylation is subject to regulation by either the Gtr pathway or the Pib2 pathway, whereas Ser3 phosphorylation primarily relies on the Pib2 pathway. As shown in the schematic.

2.2 TORC1 activation by methionine and cysteine depends mainly on the Gtr pathway and the Pib2 pathway, respectively

I explored the relationship of individual amino acids with the Gtr pathway and Pib2 pathways. To avoid bias related to auxotrophy, a prototrophic strain was prepared by introducing a plasmid expressing all auxotrophic markers[77]. I monitored the status of TORC1 activity by detecting the phosphorylation of two TORC1 substrates, Sch9 and Ser3. Following 30-min nitrogen starvation, TORC1 activity was monitored from 3 min until 12 min after stimulation with amino acids. Twenty amino acids were individually added to wild-type, *pib2*Δ, or *gtr1*Δ cells, and the cells were then harvested at various time points (Figure 2A). While Sch9 phosphorylation occurred after the addition of methionine to wild-type cells and *pib2*Δ cells (Figure 2B), it barely occurred in *gtr1*Δ cells (Figure 2B). Methionine also induced Ser3 phosphorylation in wild-type cells, but not in *gtr1*Δ cells (Figure 2B). In contrary, the addition of cysteine induced Sch9 phosphorylation in wild-type and *gtr1*Δ cells, but significantly decreased this phosphorylation in *pib2*Δ cell (Figure 2C). Ser3 phosphorylation was observed in *gtr1*Δ cells with the addition of cysteine (Figure 2C). These phosphorylation events were sensitive to rapamycin treatment, indicating that they are TORC1 dependent (Figure 2D, 2E). Collectively, these results suggested that methionine-induced TORC1 activation is more dependent on the Gtr pathway, while cysteine activation of TORC1 is more dependent on the Pib2 pathway.

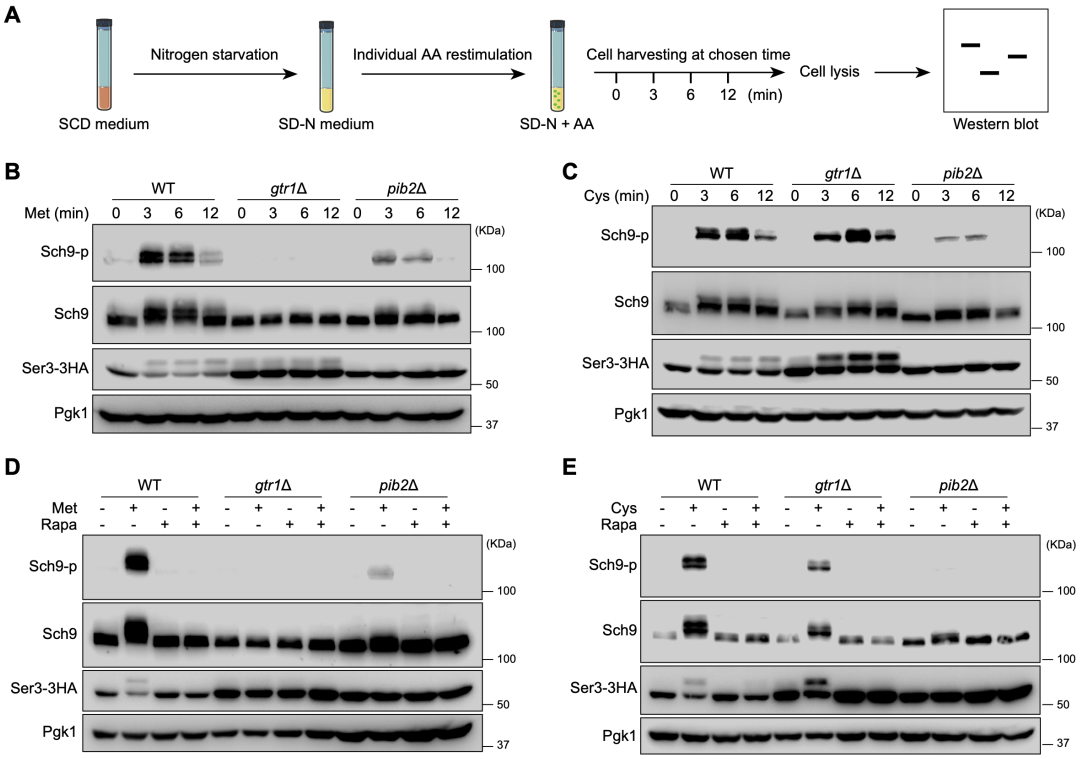

Figure 2. Methionine and cysteine activate TORC1 mainly through the Gtr and Pib2 pathways, respectively

(A) A restimulation assay of individual amino acids (AA) in wild-type (WT) (YAY2864), *gtr1*Δ (YAY2867), and *pib2*Δ (YAY2868) cells. Cells were grown in SCD medium until the exponential growth phase, shifted to SD-N medium for nitrogen starvation for 30 min, supplemented with a 5 mM concentration of each amino acid, and harvested at the indicated time points. Cell lysate were analyzed by western blotting. **(B and C)** WT (YAY2864), *gtr1*Δ (YAY2867) and *pib2*Δ (YAY2868) cells were grown as in (A), 5 mM methionine (B) or cysteine (C) was added, and the cells were harvested at the indicated time points. Lysates were analyzed by western blotting. **(D and E)** Cells (WT: YAY2864, *gtr1*Δ: YAY2867 and *pib2*Δ: YAY2868) were nitrogen starved with or without 0.2 μg/ml rapamycin for 30 min, and then methionine (D) or cysteine (E) was added for 6 min.

TORC1 localization is correlated with its activity; specifically, it is activated when distributed throughout the vacuolar membrane[28,47,72]; Under nitrogen starvation, GFP-Tor1 forms puncta proximal to the vacuolar membrane, and TORC1 activity is suppressed. When cysteine or methionine were added to starved cells, the GFP-Tor1 puncta dispersed throughout the vacuolar membrane in wild-type cells (Figure 3A). In *pib2*Δ cells, the addition of methionine decreased GFP-Tor1 puncta, but the addition of cysteine did not (Figure 3A). In *gtr1*Δ cells, on the other hand, the addition of cysteine significantly reduced the number of GFP-Tor1 puncta, whereas the addition of methionine did not (Figure 3B, 3C). The addition of cysteine decreased GFP-Tor1 puncta, which was restored by rapamycin treatment in *gtr1*Δ cells (Figure 3D, 3E). Additionally, Pib2 localization has been reported to be correlated with TORC1 activity[54]. GFP-Pib2 puncta are associated with vacuoles in *gtr1*Δ cells under nitrogen starvation, and their number decreased with the addition of cysteine but not methionine (Figure 3F, 3G). Autophagy occurs downstream of TORC1, and Atg2 is recruited to puncta called the PAS when TORC1 is inactivated during starvation[78,79,10]. When cysteine was added after starvation, the number of Atg2-GFP puncta was decreased in wild-type cells and *gtr1*Δ cells, but not in *pib2*Δ cells (Figure 3H, 3I). In contrast, the addition of methionine decreased the number of Atg2-GFP puncta in *pib2*Δ cells and wild-type cells, but not in *gtr1*Δ cells (Figure 3H, 3I).

Collectively, these results reinforce the conclusion that methionine-induced TORC1 activation is mainly dependent on the Gtr pathway, while cysteine activation of

TORC1 depends more on the Pib2 pathway.

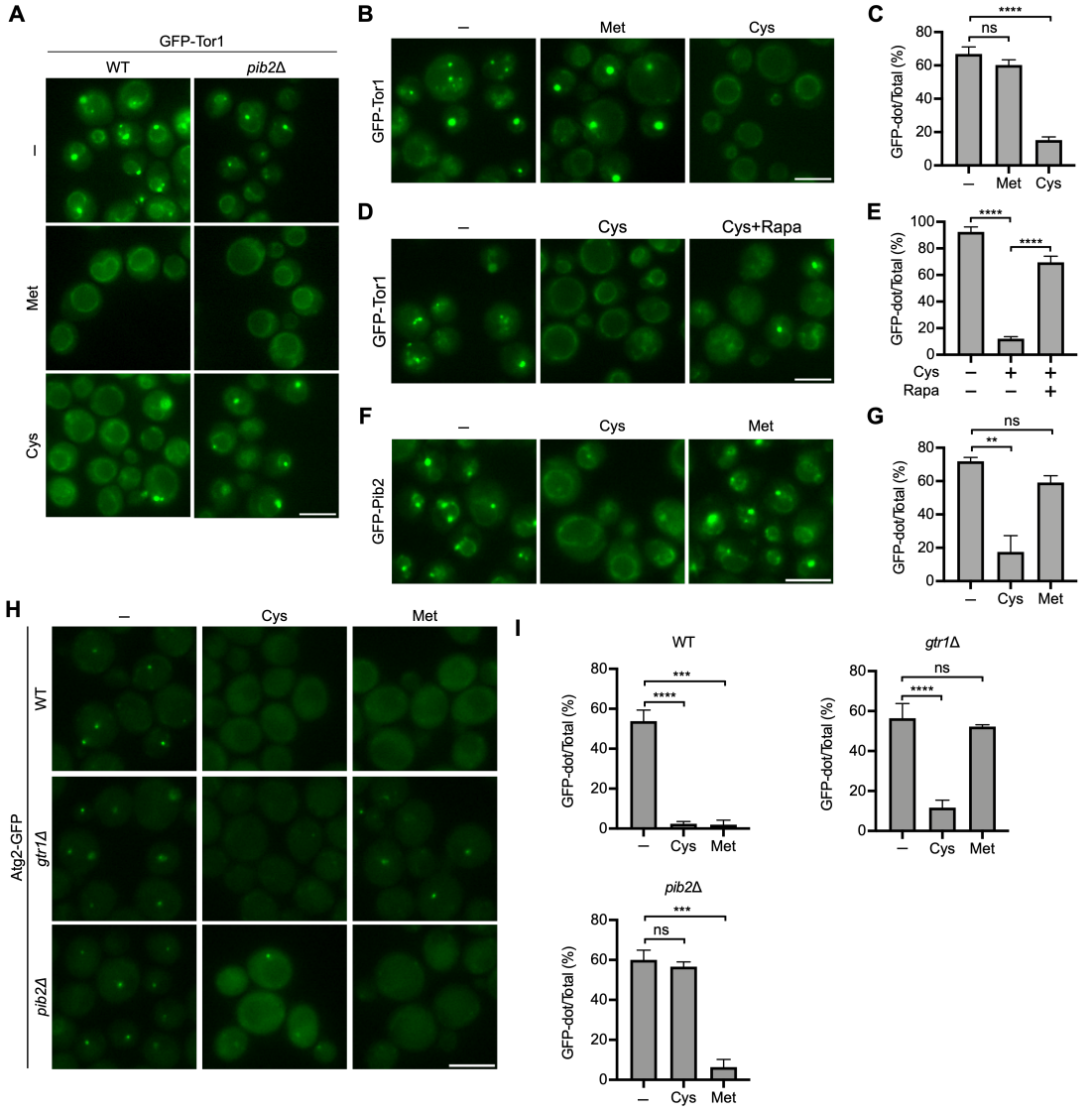

Figure 3. TORC1 is activated by methionine and cysteine via the Gtr and Pib2 pathways, respectively

(A) Cells (WT: ZQZ101, *pib2*Δ: ZQZ103) were nitrogen starved for 30 min and replenished with methionine or cysteine for 6 min. Scale bar; 5 μm. **(B and C)** *gtr1*Δ cells expressing GFP-Tor1 (ZQZ102) were cultured as in (A). Scale bar; 5 μm. The percentages of cells with vacuolar membrane-associated GFP-Tor1 puncta were calculated in (C). The graph shows the means ± SD from three independent experiments (n > 60). Unpaired *t*-test. ns, no significance, **** $P < 0.0001$. **(D and E)** Cells (ZQZ102) were nitrogen starved with or without 0.2 μg/mL rapamycin for 30 min, then adding cysteine for 6 min. Scale bar; 5 μm. (E) The percentage of cells exhibiting GFP-Tor1 puncta associating with the vacuole were calculated. The graph represents means ± SD from three independent experiments (n > 60). Unpaired *t*-test. **** $P < 0.0001$. **(F and G)** Cells (ZQZ114) were cultured as in (A). Scale bar; 5 μm. The percentage of cells with GFP-Pib2 puncta were calculated in (G). The data represent means ± SD from three

independent experiments (n > 65). Unpair *t*-test. ns, no significance, ** P < 0.01. **(H and I)** *gtr1*Δ cells expressing Atg2-GFP (WT: ZQZ148, *gtr1*Δ: ZQZ150, *pib2*Δ: ZQZ152) were cultured as in (A). Scale bar; 5 μm. The percentage of cells exhibiting Atg2-GFP puncta was calculated in (I). The graph represent means ± SD from three independent experiments (n > 55). Unpaired *t*-test. ns, no significance, *** P < 0.001, **** P < 0.0001.

2.3 Amino acid differ in their dependencies on the Gtr and Pib2 pathways in TORC1 activation

I next examined amino acids other than methionine and cysteine. In the case of lysine, the phosphorylation level of Sch9 was significantly decreased in both *gtr1*Δ cells and *pib2*Δ cells (Figure 4A), suggesting that lysine activates TORC1 through both Gtr and Pib2 pathways.

Serine was able to induce Sch9 phosphorylation in wild-type cells (Figure 4B). Even in *gtr1*Δ or *pib2*Δ cells, Sch9 was phosphorylated with the addition of serine, and Ser3 was phosphorylated in *gtr1*Δ cells (Figure 4B). Based on this result, I considered it possible that serine activated TORC1 through a third pathway. However, when both Gtr and Pib2 pathways were simultaneously abrogated in *gtr1*Δ *ego1*Δ with temperature-sensitive *pib2* cells[54], serine did not induce phosphorylation of Sch9 and Ser3 at restrictive temperature of 37 °C (Figure 4C). These results indicates that serine can activate TORC1 by either the Gtr or Pib2 pathway.

Based on these criteria, 20 amino acids were divided into four types. **Type 1**: amino acids more dependent on Gtr pathway: Met, Leu, Ile, Glu, Asp, His, Phe, Tyr, and Trp. As shown in the case of Met (Figure 2B), a Sch9 phosphorylation was induced by these amino acids in *pib2*Δ cells, but only minimally in *gtr1*Δ cells (Figure 4D, 4E). These amino acids did not induce significant Ser3 phosphorylation in *gtr1*Δ cells (Figure 2B, 5A, 5B). **Type 2:** amino acids more dependent on Pib2 pathway: Cys, Gly, Gln, Val and

Ala. As shown in the case of Cys (Figure 2C), Sch9 phosphorylation occurred in *gtr1*Δ cells but was significantly reduced in *pib2*Δ cells (Figure 4D, 4E). These amino acids also efficiently induced Ser3 phosphorylation in *gtr1*Δ cells (Figure 2C, 5A, 5B). **Type 3**: amino acids dependent on both the Gtr and Pib2 pathways: Lys, Pro and Arg. As shown in the case of Lys (Figure 4A), Sch9 phosphorylation was significantly decreased in *gtr1*Δ cells and *pib2*Δ cells compared to wild-type cells (Figure 4D, 4E). These amino acids did not significantly induce Ser3 phosphorylation in *gtr1*Δ cells (Figure 4A, 5A, 5B). **Type 4**: amino acids dependent on either the Gtr or Pib2 pathway: Ser, Asn, and Thr. As shown in the case of Ser (Figure 4B), Sch9 was efficiently phosphorylated in both *gtr1*Δ cells and *pib2*Δ cells (Figure 4D, 4E). These amino acids also efficiently induced Ser3 phosphorylation in *gtr1*Δ cells (Figure 4B, 5A, 5B). I confirmed that Asn and Thr did not induce Sch9 or Ser3 phosphorylation in *gtr1*Δ *ego1*Δ with temperature-sensitive *pib2* cells at 37 °C (Figure 5C, 5D).

Collectively, these data suggest that there are differences between amino acids regarding their dependencies on the two pathways of TORC1 activation (Figure 5E).

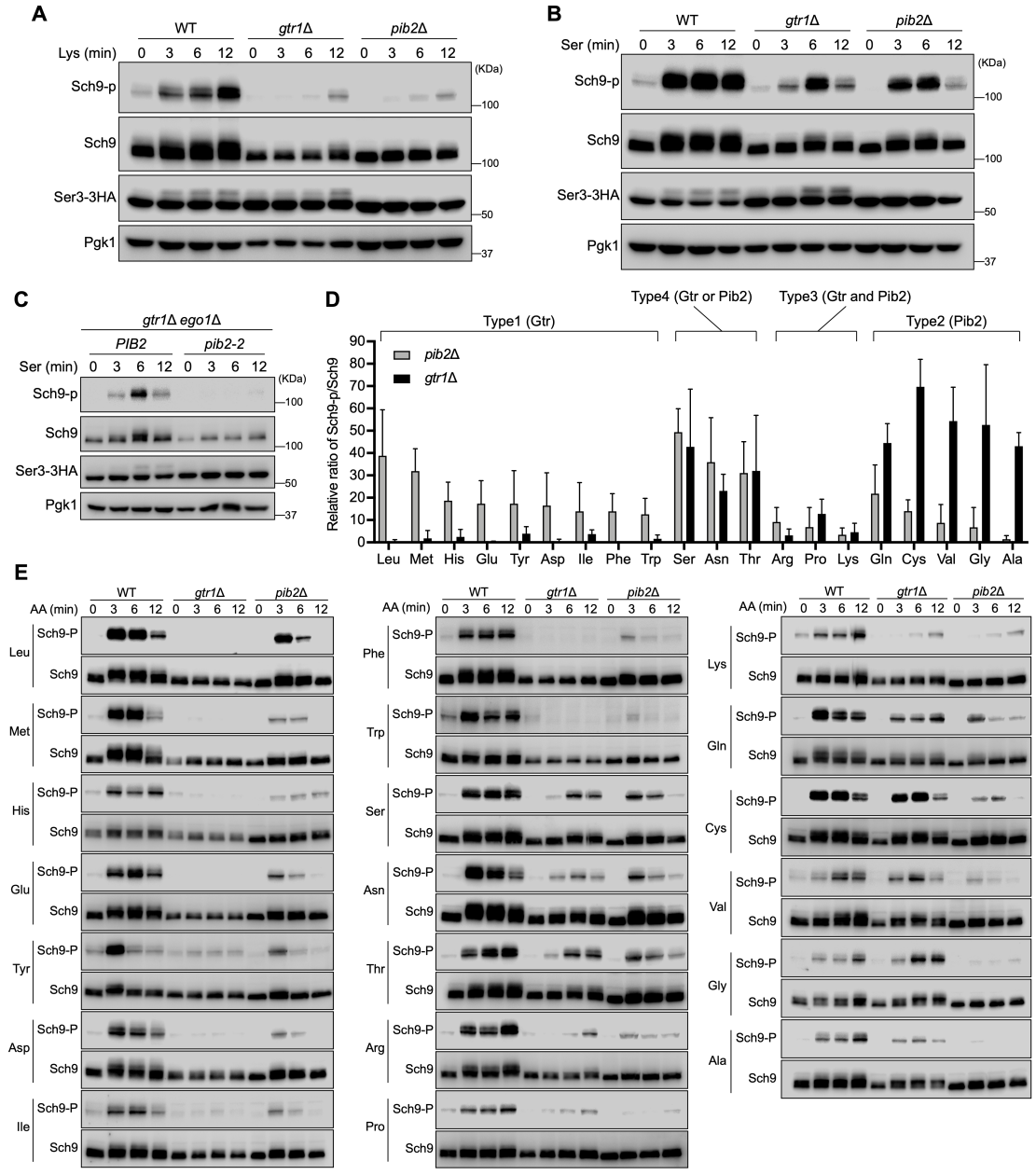

Figure 4. Classification of each amino acid according to dependency of the Gtr and Pib2 pathways

(A and B) WT (YAY2864), *gtr1*Δ (YAY2867) and *pib2*Δ (YAY2868) cells were grown as in Figure 2A; 5 mM lysine (A) or serine (B) was added, and the cells were harvested at the indicated time points. Lysates were analyzed by western blotting. **(C)** *gtr1*Δ *ego1*Δ cells (*PIB2*: ZQZ108 or *pib2-2*: ZQZ109) expressing Ser3-3HA were nitrogen starved for 30 min and cultured with serine at 37 °C at the indicated time points. **(D)** Cells (YAY2864, YAY2867, and YAY2868) were cultured as in Figure 2A, and a 5 mM of each amino acid was added. See Figure (E) for immunoblotting data. The average band intensities of Sch9 phosphorylation at 3 min and 6 min relative to the band intensities of Sch9 are presented. The mean ± SD of three independent biological replicates are shown. **(E)** Cells

(YAY2864, YAY2867 and YAY2868) were cultured as in Figure 2A, 5 mM indicated amino acid was added, and the cells were harvested at the indicated time points. Lysates were analyzed by western blotting using anti-Sch9-p (T737) and anti-Sch9 antibodies.

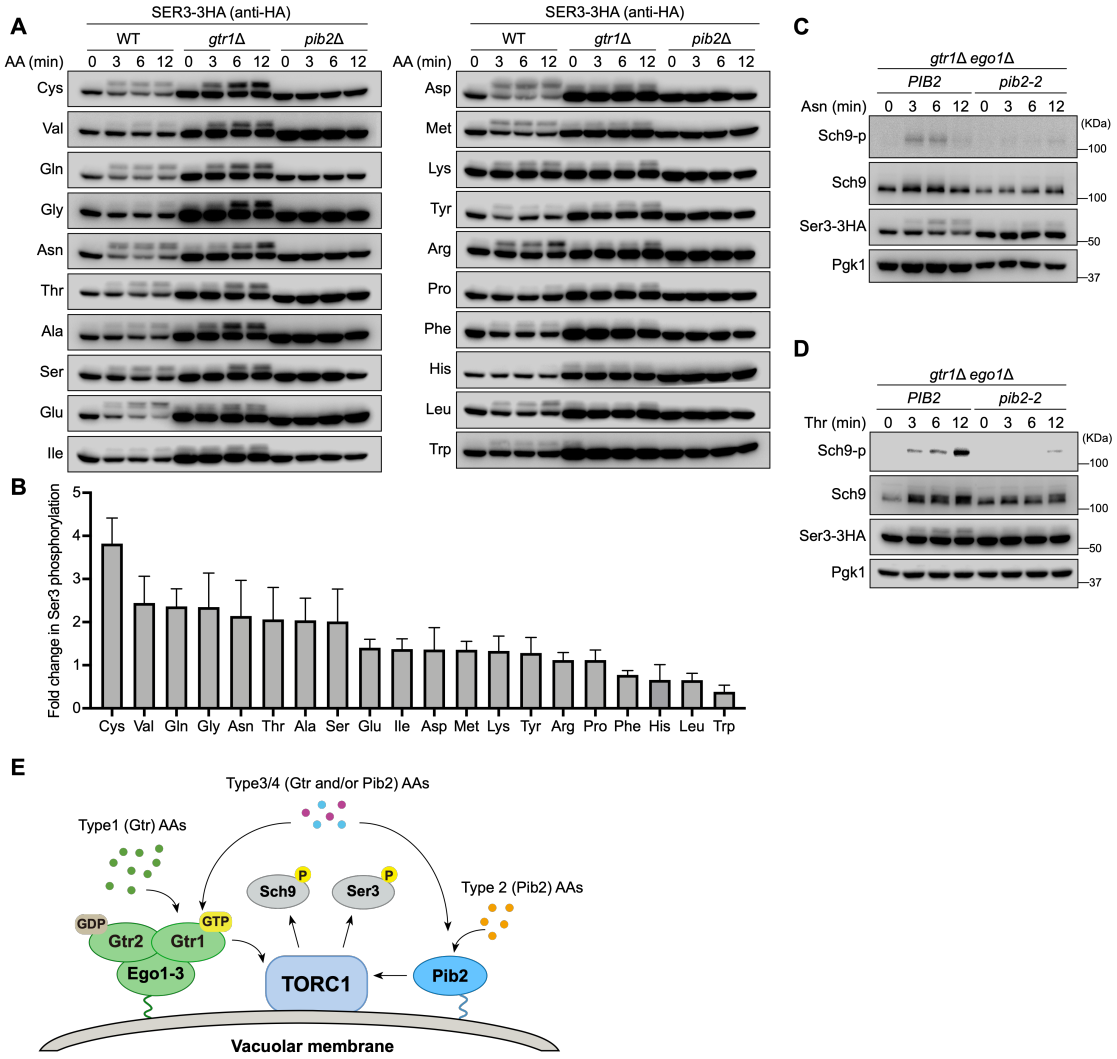

Figure 5. Distinct Amino Acid Species Preferences of the Gtr and Pib2 Pathways for TORC1 Activation

(A) Cells (YAY2864, YAY2867, and YAY2868) were subjected as Figure 4E and analyzed by western blotting using anti-HA antibodies. **(B)** Cells (YAY2864, YAY2867, and YAY2868) were cultured as in Figure 2A, and added with 5 mM of each amino acid. The fold change of Ser3 phosphorylation at the average of three different time points (3, 6, and 12 min) relative to wild type (YAY2864) is shown for each amino acid. Immunoblotting data are shown in (A). The data represent the mean ± SD of three independent biological replicates. **(C and D)** Cells (ZQZ108 or ZQZ109) were cultured and analyzed as in Figure 4C. **(E)** Amino acids shown in green activate TORC1 via the Gtr pathway. Amino acids shown in orange activate TORC1 via the Pib2 pathway. Amino acids shown in blue activate TORC1 via both Gtr and Pib2 pathways. Amino acids shown in purple activate TORC1 via the Gtr or Pib2 pathway.

2.4 Cysteine activates TORC1 via the Pib2 pathway

Of the aforementioned results, I focused on the fact that cysteine exerted the most prominent effect on TORC1 activation in *gtr1*Δ cells (Figure 4D, 5B). This was based on a comparison of the responses of wild-type and *gtr1*Δ cells to each amino acid. In order to compare each amino acid more directly, I observed the response in *gtr1*Δ cells to all amino acids in the same blot. After nitrogen starvation, each amino acid was added individually for 6 min. Type 2 (Pib2) and Type 4 (Gtr or Pib2) amino acids induced Sch9 and Ser3 phosphorylation, which were inhibited by rapamycin treatment in *gtr1*Δ cells (Figure 6A, 6B, 6C, 6D). In agreement with the previous results, cysteine resulted in the most significant phosphorylation of both Sch9 and Ser3 in *gtr1*Δ cells (Figure 6A, 6B).

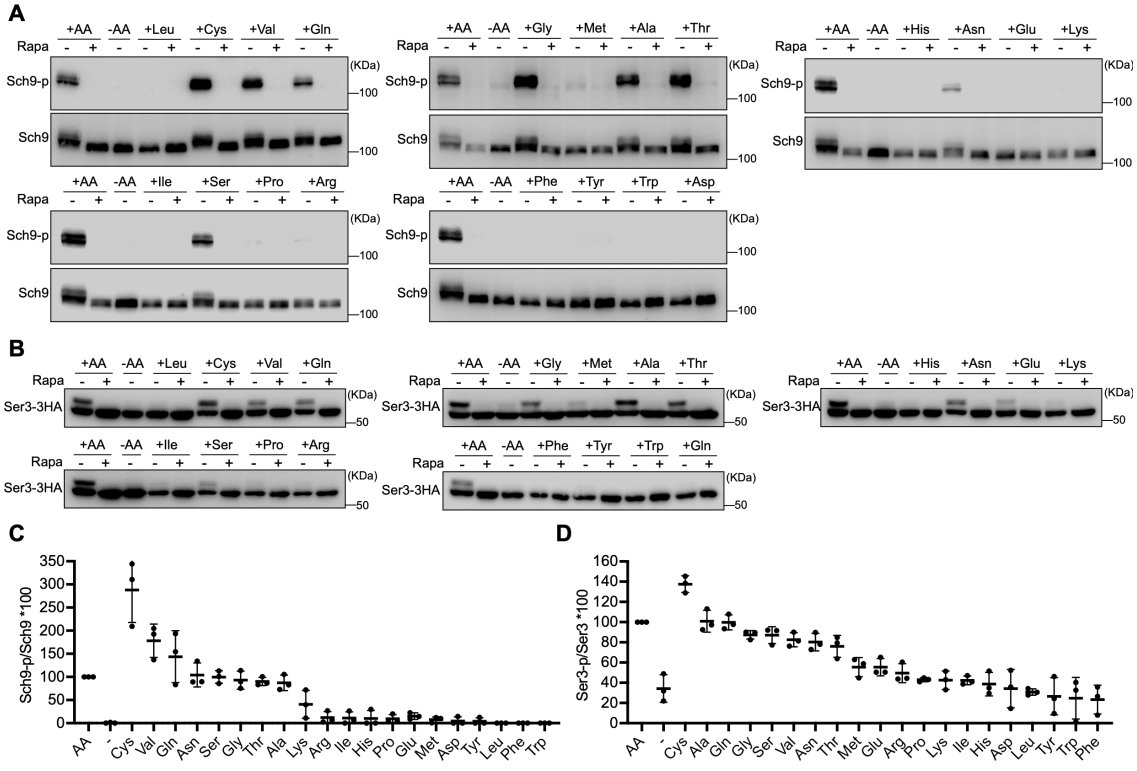

Figure 6. The ability of 20 individual amino acids to activate TORC1 through the Pib2 pathway

(A and B) Cells (YAY2867) were nitrogen starved with or without 0.2 μg/mL rapamycin for 30 min, and then incubated with complete amino acids (+AA), without amino acids (-AA) or individual amino acids were added for 6 min. Lysates were analyzed by western blotting using anti-Sch9 and anti-Sch9-p in (A) and using anti-HA in (B). **(C and D)** *gtr1*Δ cells (YAY2867) were culture as in (A and B). See (A) and (B) for immunoblotting data. The ratio of the band intensity of Sch9-p/Sch9 (A) and Ser3-p/Ser3 (B) of each amino acid relative to that of complete amino acids (AA). The mean ± SD of three independent biological replicates is shown.

Likewise, the formation of GFP-Tor1 puncta under nitrogen starvation was more effectively decreased by cysteine than by any of the other Type 2 amino acids, including glutamine, as our group previously reported (Figure 7A)[54]. The formation of GFP-Tor1 puncta was also decreased by the re-addition of cysteine within 6 min after nitrogen starvation, and it gradually resumed over time (Figure 7B, 7C). A time-course analysis of cysteine-induced TORC1 activation showed that Sch9 and Ser3 phosphorylation peaked at 6 min after cysteine addition, then started to decrease (Figure 7D). A concentration-dependency analysis showed that the addition of 50-100 μM cysteine induced minimal TORC1 activity, and this activity was mostly saturated at 5 mM (Figure 7E).

There is a possibility that *pib2*Δ cells do not sufficiently take up cysteine from the medium, leading to impaired TORC1 activation. In fact, it has been reported that Gtr affects the functional localization of Gap1, a general amino acid permease, at the plasma membrane[80,81]. To assess this possibility, I confirmed that Gap1-GFP and Yct1-GFP (Yct1 is a high-affinity cysteine-specific transporter)[82,83] localized normally at the plasma membrane in both *pib2*Δ cells and wild-type cells (Figure 7F, 7G). Further, measured [^{35}S]-cysteine uptake into cells. As controls, *gap1*Δ cells and *yct1*Δ cells, obviously reduced cysteine uptake (Figure 7H). However, *pib2*Δ cells did not exhibit defective uptake (Figure 7H). These results ruled out the possibility that the defective cysteine-induced TORC1 activation in *pib2*Δ cells is due to inefficient cysteine uptake.

Glutathione is a downstream metabolite of cysteine. To determine whether

TORC1 is activated indirectly after converted into glutathione, I examined a deletion mutant of gamma glutamylcysteine synthetase, encoded by *GSH1*, which catalyzes the first step in glutathione (GSH) biosynthesis[84]. However, cysteine-dependent TORC1 activation was not affected in *gsh1*Δ cells, and glutathione addition did not promote TORC1 activation (Figure 7I). These indicated that the activation of TORC1 by cysteine is not mediated through its conversion into glutathione.

Altogether, these data indicate that cysteine-induced TORC1 activation employs primarily the Pib2 pathway.

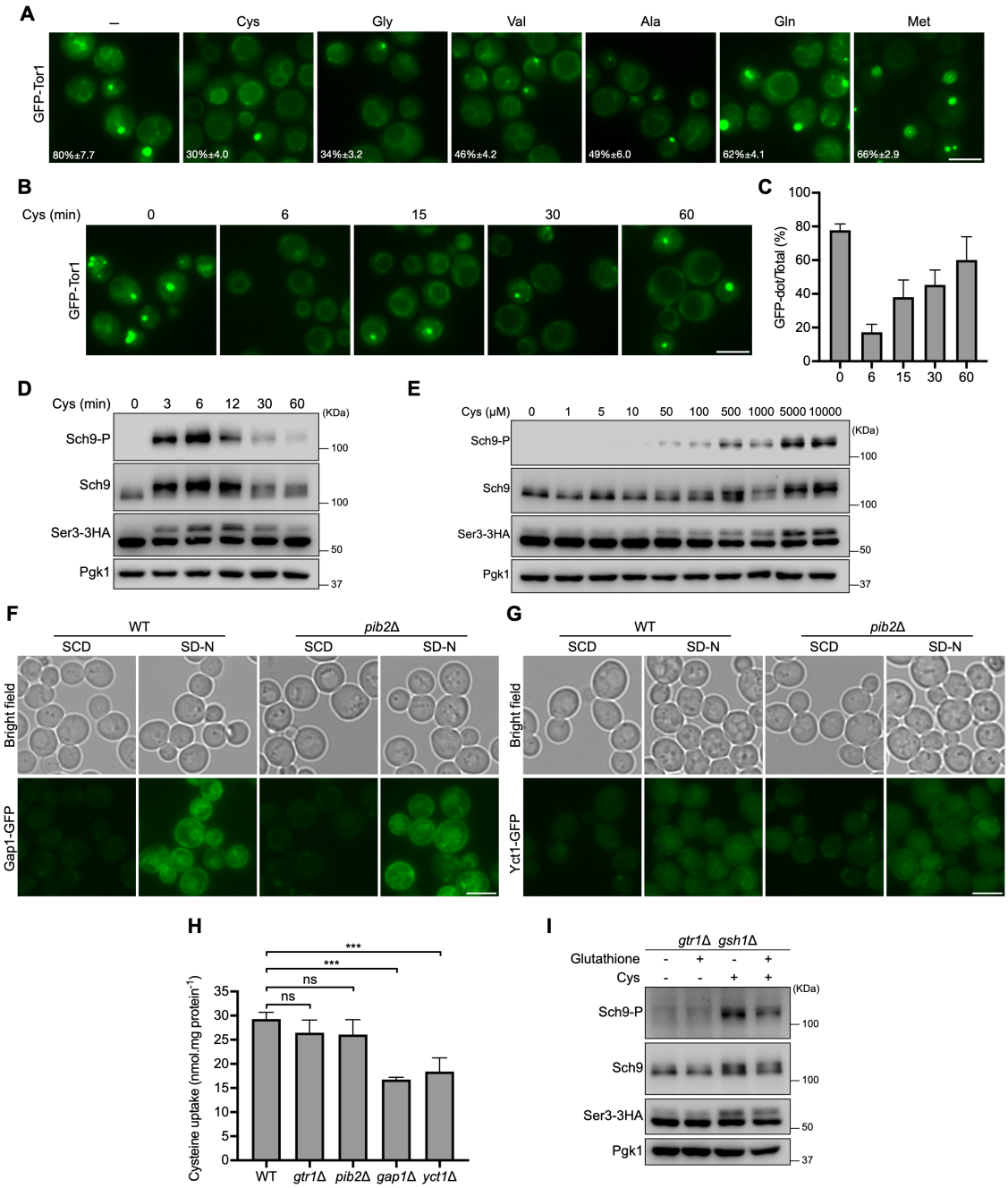

Figure 7. Cysteine activates TORC1 through Pib2 pathway

(A) Cells (ZQZ102) were culture as in Figure 2D. Scale bar; 5 μm. **(B and C)** Cells (ZQZ102) were starved of nitrogen for 30 min and replenished with 5 mM cysteine for indicated time. Scale bar; 5 μm. Percentage of cells exhibiting GFP-Tor1 puncta associating with the vacuole were calculated in (C). The data represent means ± SD from three independent experiments (n > 70). **(D)** Cells (YAY2867) were starved of nitrogen for 30 min, and replenished with 5 mM cysteine, and harvested at indicated time point. **(E)** Cells (YAY2867) were nitrogen-starved for 30 min and restimulated with cysteine at the indicated concentrations for 6 min. Lysates were analyzed by immunoblotting. **(F and**

G) Cells expressing Gap1-GFP (WT: ZQZ137, *pib2*Δ: ZQZ138) and Yct1-GFP (WT: ZQZ146, *pib2*Δ: ZQZ147) were grown in SCD medium, and then starved of nitrogen for 30 min. **(H)** Cells (WT: YAY2864, *gtr1*Δ: YAY2867, *pib2*Δ: YAY2868, *gap1*Δ: ZQZ232, *yct1*Δ: ZQZ233) were starved of nitrogen for 30 min and then added with 0.5 μM L-[^{35}S]cysteine and incubated for 5 min. The cells were collected, and the amount of intracellular L-[^{35}S]cysteine was determined. The graph represents means ± SD from three independent experiments. Unpaired *t*-test. ns, no significance, *** $P < 0.001$. **(I)** Upon nitrogen starvation, cells (ZQZ118) were treated with or without 5 mM cysteine or glutathione for 6 min.

2.5 Cysteine promotes Pib2-TORC1 interaction *in vivo*

Since previous studies showed that Pib2 associates with TORC1[53,54], I investigated whether cysteine affects the interaction. The amount of Tor1 that co-precipitated with GFP-Pib2 was greater after the addition of cysteine to the medium than in cells under starvation conditions (Figure 8A). By contrast, the interaction between Gtr1 and TORC1 was not enhanced by cysteine addition (Figure 8B). The inclusion of cysteine in lysis buffer also enhanced this interaction (Figure 8C). When cysteine was added to immunoprecipitation buffers, Pib2-Tor1 interaction was further promoted in a dose-dependent manner (Figure 8D). Leucine, a Type 1 (Gtr) amino acid, did not enhance this interaction (Figure 8E).

Although D-cysteine shares chemical properties with its enantiomer L-cysteine, only L-cysteine is utilized in cellular processes, including TORC1 activation via the Pib2 pathway (Figure 8F). Consistently, D-cysteine did not promote Pib2-TORC1 interaction unlike L-cysteine (Figure 8G). The addition of cysteine to all immunoprecipitation assay buffers enhanced Pib2-TORC1 interaction in a dose-dependent manner (Figure 9A, 9B), whereas D-cysteine and L-methionine did not (Figure 9C, 19D). These results suggest that L-cysteine enhanced Pib2-TORC1 interaction quite specifically.

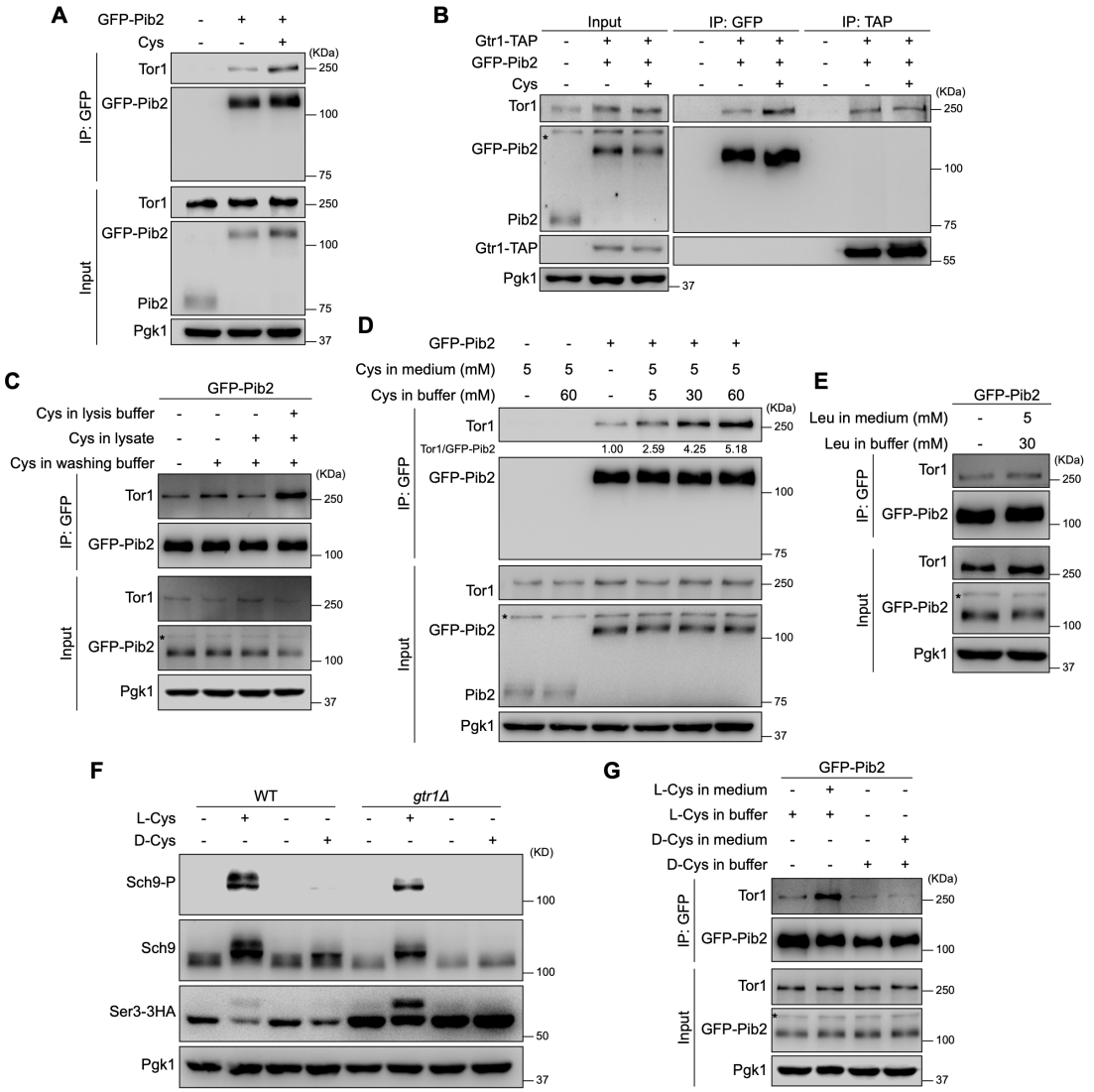

Figure 8. Cysteine promotes Pib2-TORC1 interaction *in vivo*

(A) Cells (ZQZ114) were nitrogen starved for 30 min, then incubated with or without 5 mM cysteine for 15 min. Cellular extracts were immunoprecipitated by GFP-Trap. Whole-cell extract and precipitated proteins were analyzed by western blotting using anti-Tor1, anti-Pib2, anti-Pgk1 antibodies. **(B)** Cells (ZQZ116) were cultured as in (A). Extracts were prepared and immunoprecipitated by GFP-Trap or IgG-Dynabeads. Whole-cell extract and precipitated proteins were analyzed by immunoblotting using anti-Tor1, anti-Pib2, anti-TAP, and anti-Pgk1antibodies. The asterisk indicates non-specific band. **(C)** Cells (ZQZ114) were nitrogen starved restimulated with 5 mM cysteine and the lysates were immunoprecipitated with GFP-Trap. The immunoprecipitation lysis buffer, cell lysate, and washing buffer were supplemented with 30 mM cysteine. **(D)** Cells (ZQZ114) were treated as in (A) and the indicated concentrations of cysteine were added to the immunoprecipitation buffer. The asterisk indicates non-specific bands. **(E)** Cells (ZQZ116) were cultured as in (B). **(F)** WT (YAY2864), *gtr1*Δ (YAY2867) cells were nitrogen starved for 30 min, then incubated for 6 min after the addition of 5 mM L- or D-

cysteine. **(G)** Cells (ZQZ114) were subjected to 30 mM L-cysteine or D-cysteine in the immunoprecipitation buffer, as in (D). The asterisk indicates non-specific bands.

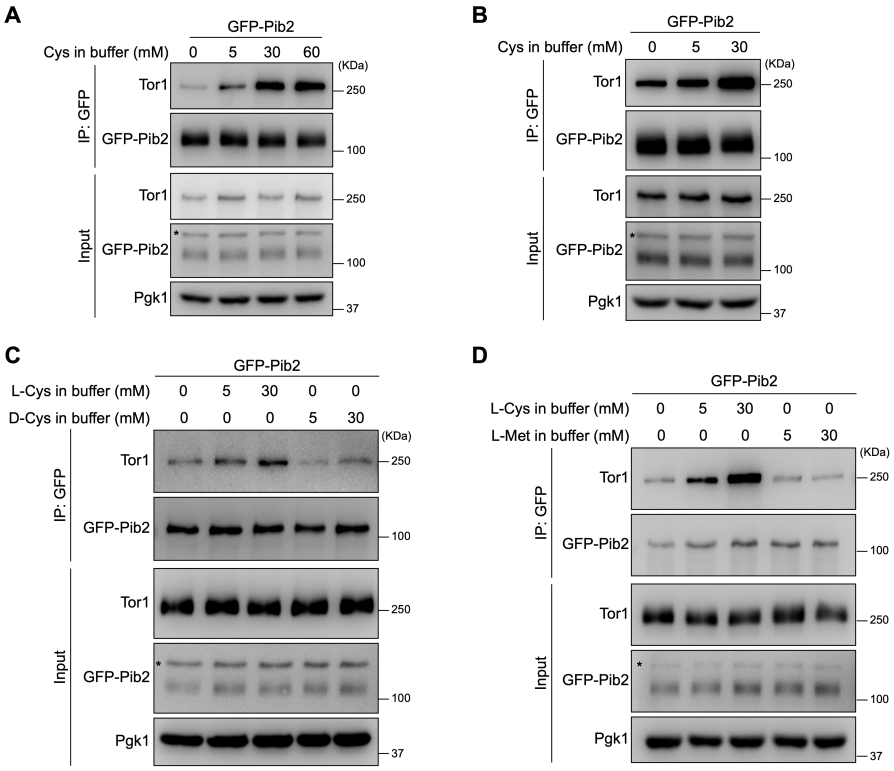

Figure 9. Cysteine enhances Pib2-TORC1 interaction *in vitro*

(A) Cells (ZQZ114) were nitrogen starved for 30 min. Extracts were prepared and immunoprecipitated with GFP-Trap, and then the indicated concentrations of cysteine were added to the immunoprecipitation buffer. **(B)** Cells (ZQZ114) were culture in YPD medium. Extracts were treated as in (A). **(C and D)** Cells (ZQZ114) were cultured as in (A), and the indicated concentrations of amino acids were added to the immunoprecipitation buffer.

2.6 Cysteine directly promotes Pib2-TORC1 interaction *in vitro*

To identify additional factors involved in this cysteine-dependent process, I analyzed proteins that co-immunoprecipitated with GFP-Pib2, with or without cysteine addition, followed by liquid chromatography–tandem mass spectrometry (LC-MS/MS) (Figure 10A). Consistent with the above results, GFP-Pib2 co-immunoprecipitated all the subunits of TORC1, namely Tor1, Tor2, Kog1, Tco89, and Lst8, and their amounts were increased with the addition of cysteine (Figure 10B). Following LC-MS/MS, I selected the other 55 proteins whose amounts changed upon cysteine addition (Figure 10C), and analyzed the effects of their deletion on the activation of TORC1 by cysteine. However, no factors affecting the cysteine-dependent response were identified (data not shown).

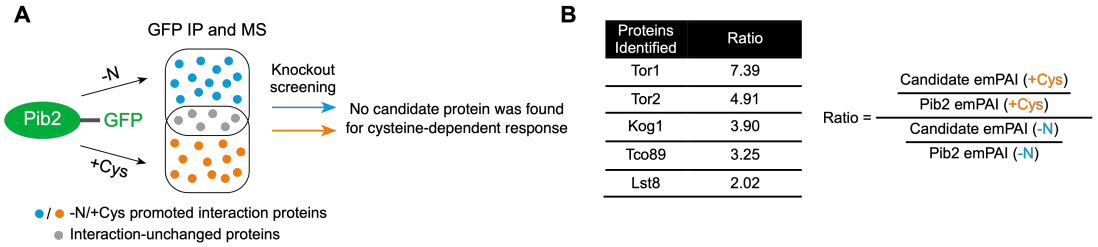

B

Proteins Identified	Ratio
Tor1	7.39
Tor2	4.91
Kog1	3.90
Tco89	3.25
Lst8	2.02

$$\text{Ratio} = \frac{\dfrac{\text{Candidate emPAI (+Cys)}}{\text{Pib2 emPAI (+Cys)}}}{\dfrac{\text{Candidate emPAI (-N)}}{\text{Pib2 emPAI (-N)}}}$$

C

-N promoted interaction proteins

Candidates	Ratio
ALT1	$0/3.44*10^4$
STU2	$0/4.31*10^4$
OSH7	$0/4.33*10^4$
COG6	$0/4.50*10^4$
RPN9	$0/4.73*10^4$
MRPL35	$0/5.06*10^4$
OTU1	$0/6.53*10^4$
MRPL13	$0/7.24*10^4$
PUP2	$0/7.65*10^4$
YNR029C	$0/8.88*10^4$
RPS30B	$0/3.40*10^3$
RPS18B	0.41
RBG2	0.71
HIS4	0.83
NSR1	0.83
RPS7A	0.98

+Cys promoted interaction proteins

Candidates	Ratio
PAB1	$4.85*10^2/0$
RPL4B	$1.64*10^2/0$
ARF2	$1.40*10^2/0$
RLP7	$1.07*10^3/0$
KES1	$1.06*10^3/0$
HHO1	$9.09*10^4/0$
LAT1	$7.26*10^4/0$
RPN11	$7.22*10^4/0$
ERG10	$5.87*10^4/0$
LSM4	$5.62*10^4/0$
YHB1	$5.46*10^4/0$
TMA22	$5.30*10^4/0$
SFM1	$4.81*10^4/0$
HSN1	$4.38*10^4/0$
RPN10	$3.98*10^4/0$
AIM45	$3.19*10^4/0$
PRP39	$3.18*10^4/0$
TAL1	$3.18*10^4/0$
WRS1	$2.37*10^4/0$

+Cys promoted interaction proteins

Candidates	Ratio
ASN1	7.17
MSH2	4.87
SAM2	3.23
APM3	3.09
EIS1	2.93
YLR419W	2.24
ILV1	2.00
TRP5	1.69
ARF1	1.59
MDH3	1.57
RPL12A	1.51
IMD2	1.51
RPS25A	1.50
RPS5	1.49
PET9	1.49
LSM12	1.44
PBP1	1.35
RPL9B	1.25
RPL9A	1.25
STM1	1.18

Figure 10. Cysteine enhances Pib2 interacting with TORC1 subunits

(A) Schematic illustration of the identification of cysteine-sensitive Pib2-interacting proteins by immunoprecipitation and mass spectrometry analysis. **(B)** The relative abundance of proteins identified in GFP-Pib2 (ZQZ114) purifications is compared between buffers with or without 30 mM of cysteine, which is calculated as in the indicated formula of Ratio. **(C)** Cysteine-dependent identification of Pib2-interacting proteins through immunoprecipitation and mass spectrometry analysis.

Based on this outcome, I hypothesized that cysteine may activate TORC1 via Pib2 without additional factors. I then aimed to perform pull-down assay with recombinant Pib2 proteins *in vitro*, but did not obtain a sufficient amount of full-length recombinant Pib2 protein. Therefore, I sought to identify the region of Pib2 that is required for the cysteine-dependent activation of TORC1 in yeast. Pib2 is a 635-amino-acid protein that contains two highly conserved motifs, namely the FYVE domain and the tail (T) motif, as well as five motifs, designated A to E, that are weakly evolutionally conserved (Figure 11A)[51]. In cells expressing a series of truncated Pib2 fused to GFP in *pib2*Δ cells, the addition of cysteine failed to activate TORC1 in GFP-Pib2(440-635) lacking motifs A to E (Figure 11A, 11B). Cysteine addition did not activate TORC1 in GFP-Pib2(1-620)-expressing cells, which lack the T motif (Figure 11A, 11B). However, GFP-Pib2(304-635), which contains only amino acids from the E motif to the T motif responded to cysteine activation of TORC1 (Figure 11A, 11B). These data indicated that the region from the E motif to the T motif of Pib2 are necessary and sufficient for TORC1 activation by cysteine.

Hence, I purified GST-Pib2(304-635) from *E. coli*, which resulted in improved solubility and stability of the recombinant Pib2 protein (Figure 11C). I also purified TAP-Tor1 from a yeast strain (Figure 11C), and incubated it with GST-Pib2(304-635) *in vitro* with or without cysteine. TAP-Tor1 did not co-precipitate GST-Pib2(304-635) without cysteine, but cysteine supplementation facilitated the association of GST-Pib2(304-635) with TAP-Tor1 (Figure 11D). The addition of D-cysteine or L-methionine did not

promote this interaction (Figure 11E). The Pib2(304-635)-TORC1 interaction was enhanced in a cysteine dose-dependent manner *in vitro* (Figure 11F). These results demonstrate that this cysteine-induced interaction in *vitro* requires the presence of only Pib2 and TORC1.

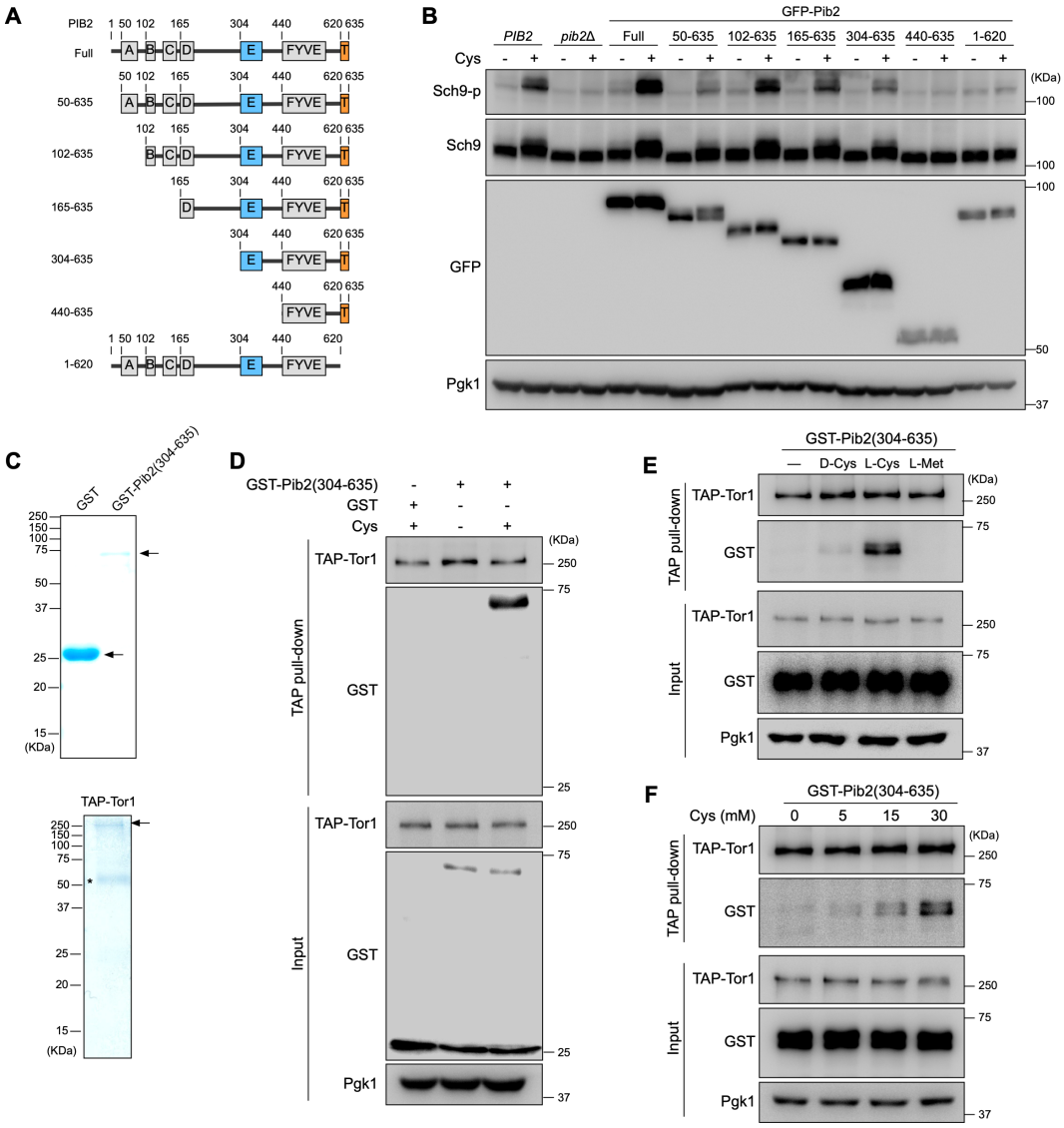

Figure 11. Cysteine directly promotes the interaction between Pib2 and TORC1 *in vitro*

(A) Schematic diagram of Pib2 with defined motifs and the truncation mutants. **(B)** WT (BY4741), *pib2*Δ cells (HUY28A), and cells expressing each *PIB2* truncation mutants (YAY2569, YAY2575, YAY2570, YAY2571, YAY2572, YAY2573, YAY2574) were nitrogen starved for 30 min, and then 5 mM cysteine was added for 6 min. **(C)** GST alone (as control) or GST-Pib2(304-635) was purified from *E. coli* and TAP alone (as control) or TAP-Tor1 was purified from yeast (ZQZ230, ZQZ231); and were then subjected to SDS-PAGE and stained with CBB. The asterisk indicates non-specific bands. **(D)** Lysates from yeast cells (ZQZ230) expressing TAP-tagged Tor1 were immunoprecipitated by IgG-Dynabeads. Beads conjugated to TAP-Tor1 were incubated with purified GST-Pib2(304-635), with or without 30 mM cysteine for 3 h at 4 °C, then subjected to TAP pull-down assay. **(E)** TAP pull-down assay with or without 30 mM concentrations of indicated amino acids, as in (D). **(F)** TAP pull-down assay with indicated concentration

of L- cysteine, as in (D).

2.7 Cysteine binds directly to Pib2

Given the above results, I hypothesized that cysteine might bind directly to Pib2. To examine this possibility, I performed an equilibrium binding assay *in vitro*[73]. Radiolabeled cysteine was added to purified GST-Pib2(304-635), and it bound to GST-Pib2(304-635) but not to control GST protein (Figure 12A). Excess non-radiolabeled cysteine competed for this binding (Figure 12A). Serial dilution of non-labeled cysteine revealed that the dissociation constant (K_d) of the cysteine-Pib2 interaction was 136.5 μM (Figure 12B). These results established that cysteine binds directly to Pib2.

2.8 The cysteine-binding residues of Pib2 are essential for cysteine activation of TORC1

Subsequently, I sought to determine which region of Pib2 is required for the cysteine-enhanced Pib2-TORC1 interaction. Cysteine promoted the interaction of TORC1 with the GFP-Pib2(304-635), but not mutants lacking either the E motif (440-635) or lacking the T motif (304-620) (Figure 12C, 12D), indicating that both E and T motifs of Pib2 are required for the cysteine-dependent interaction with TORC1 *in vitro*. To further confirm which region of Pib2 binds to cysteine, I purified a series of GST-Pib2 truncation proteins and incubated them with radiolabeled cysteine in an equilibrium binding assay. Radiolabeled cysteine bound to GST-Pib2(440-635), which contains only

the FYVE domain and the T motif, and this binding was competitively inhibited by excess non-radiolabeled cysteine (Figure 12E). However, Pib2(304-620) lacking the T motif was unable to bind radiolabeled cysteine (Figure 12E). Taken together, these results indicate that T motif of Pib2 is critical for the binding of cysteine to Pib2.

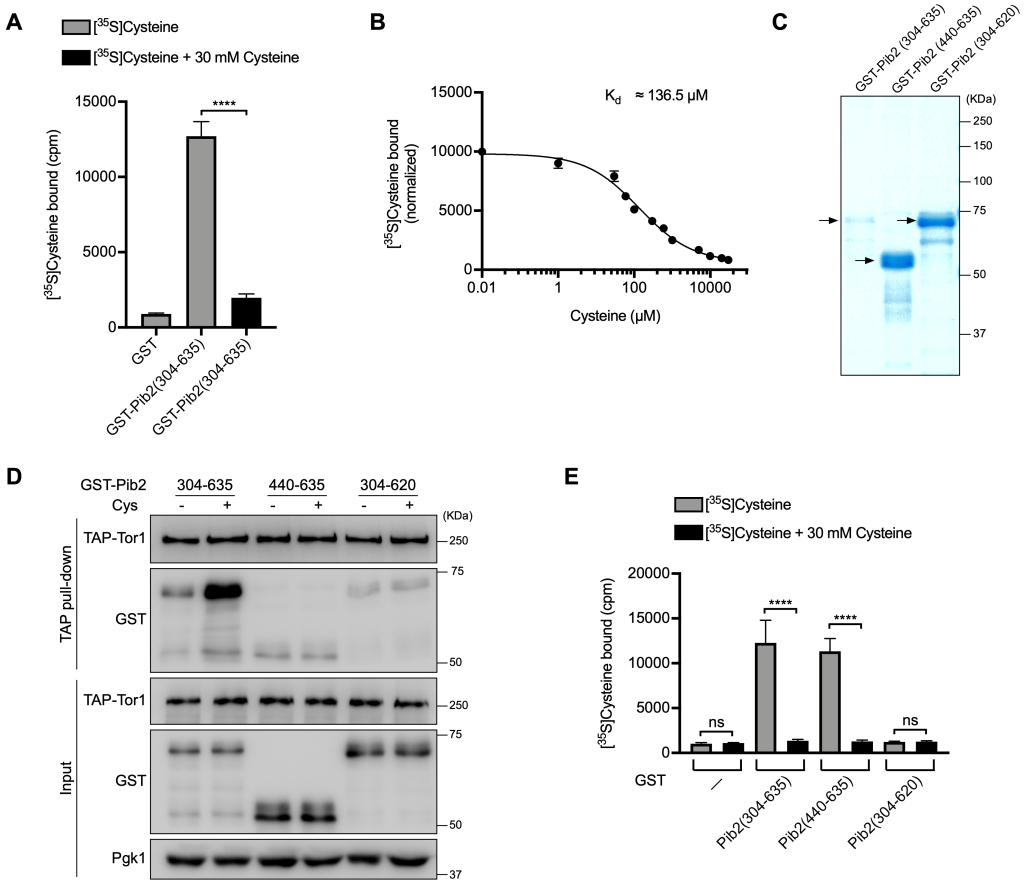

Figure 12. Cysteine directly binds to Pib2

(A) Beads binding GST and GST-Pib2(304-635) were purified from *E. coli* and incubated with 2 μCi L-[^{35}S]-cysteine, with or without unlabeled cysteine. After washed out, the radioactivity of the beads was measured. The values shown are Mean ± SD for three technical replicates from one representative experiment. Unpaired *t*-test. **** $P < 0.0001$. **(B)** GST-Pib2(304-635) was analyzed in binding assays as in (A), with 2 μCi L-[^{35}S]-cysteine and indicated concentrations of unlabeled cysteine. Each point in the graph represents the normalized mean ± SD for three technical replicates in an assay with 2 μCi L-[^{35}S]-cysteine. The K_d was calculated from the results of two independent biology replicates, each of which included three technical replicates. **(C and D)** GST-tagged Pib2 truncated proteins were prepared and analyzed by SDS-PAGE and CBB staining. TAP pull-down assay was performed as in Figure 11E. **(E)** GST-tagged proteins were prepared and cysteine-binding assays were performed and analyzed as in (A). Unpaired *t*-test. ns, no significance, **** $P < 0.0001$.

The primary sequence of T motif is well conserved in fungi (Figure 13A). To determine the critical residues in this motif, every three consecutive amino acids were replaced with three alanines (alanine was mutated to aspartic acid). As a result, the activation of TORC1 by cysteine was suppressed in cells expressing Pib2 mutants, whose residues 630-632 or 633-635 were mutated to three alanines (Figure 13B). Further alanine scanning within Pib2 residues 630-635 identified two residues, W632 and F635, which are critical for the activation of TORC1 by cysteine (Figure 13C). These residues were perfectly evolutionally conserved among the referred fungi species (Figure 13A).

Radioactive cysteine bound specifically to GST-Pib2(304-635), but this binding was significantly abolished by either W632A or F635A mutation (Figure 13D), indicating these residues are crucial for cysteine binding. The alanine substitutions in W632A and F635A significantly abrogated TORC1 activation by cysteine in yeast (Figure 13E). However, these mutations did not affect the activation of TORC1 by methionine (Type 1) or another Type 2 amino acid, glutamine (Figure 13E). After nitrogen starvation, cysteine addition led to a reduction in GFP-Pib2 puncta formation in wild type cells. However, this effect was not observed in *pib2*Δ mutants that expressed GFP-Pib2 W632A or GFP-Pib2 F635A and that lacked the entire T motif (Figure 13F, 13G). In summary, these results demonstrate that the W632 and F635 residues of Pib2 are critical for its binding to cysteine and for cysteine-dependent TORC1 activation.

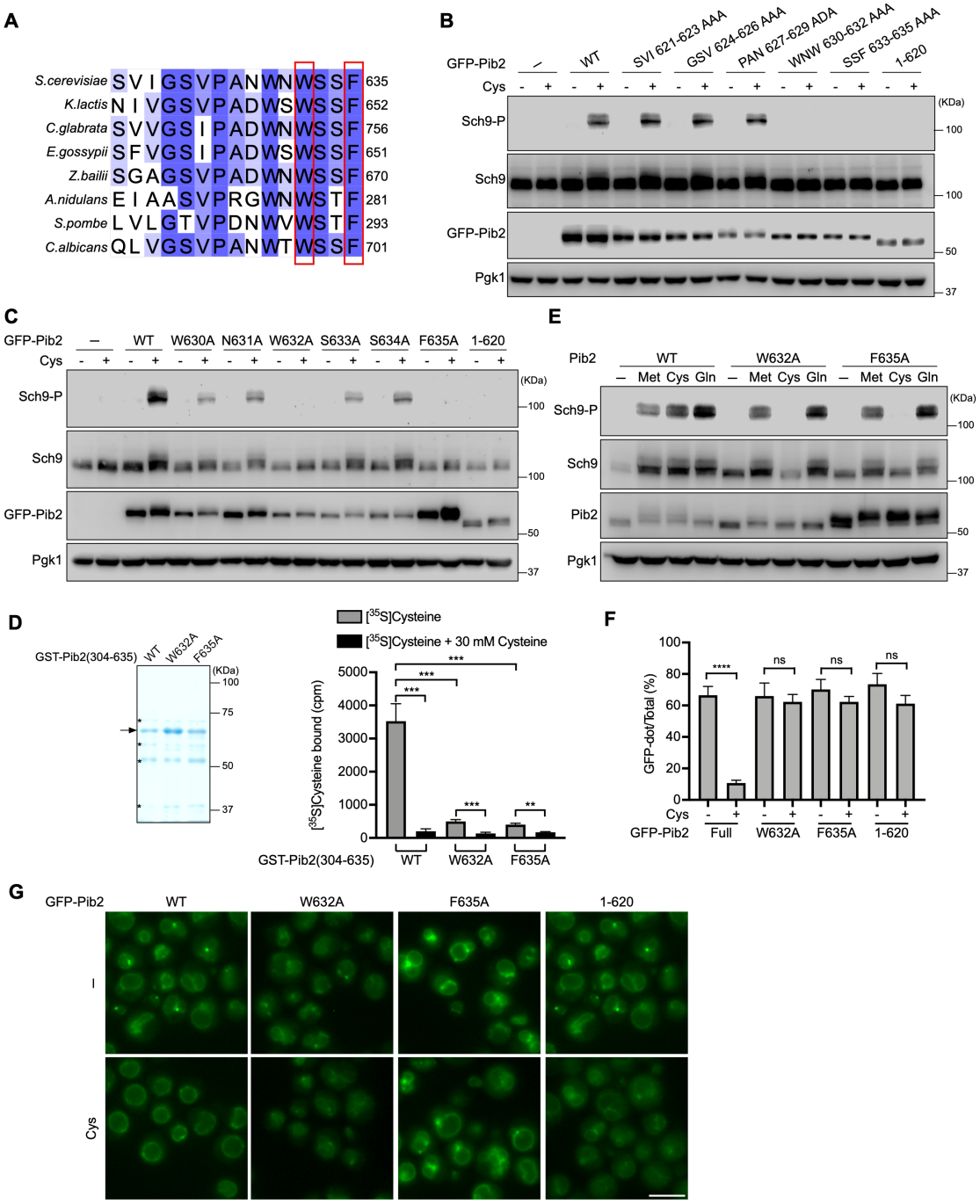

Figure 13. Pib2 W632 and F635 are essential for TORC1 activation by cysteine

(A) Alignment of the T motifs in Pib2 orthologue proteins from various fungal species. **(B)** *pib2*Δ cells (HUY28A) expressing GFP-Pib2 (YAY2569) or each Pib2 T-motif mutant (ZQZ238, ZQZ239, ZQZ240, ZQZ241, ZQZ242) were nitrogen starved for 30 min and then restimulated with or without 5 mM cysteine for 6 min. **(C)** pib2Δ cells (HUY28A) expressing GFP-Pib2 (YAY2569) or each Pib2 T-motif mutant (ZQZ253, ZQZ254, ZQZ255, ZQZ256, ZQZ257, ZQZ258, YAY2574) were subjected as in (B). **(D)** GST tagged Pib2 truncated proteins were prepared and analyzed by SDS-PAGE and CBB

staining. Cysteine-binding assays were preformed and analyzed as in Figure 6A. The arrow indicates GST-Pib2 and asterisks indicate contaminants or degradation products. Unpaired *t*-test. ** $P < 0.01$, *** $P < 0.001$. **(E)** WT cells (BY4741) or cells with Pib2 mutation W632A (ZQZ264) or F635A (ZQZ265) were analyzed as in (B). **(F and G)** *pib2*Δ cells expressing GFP-Pib2 (YAY2569) or each Pib2 T-motif mutant (ZQZ255, ZQZ258, YAY2574). Cells were cultured as in Figure 2D. Scale bar; 5 μm. The graph represent means ± SD ($n > 70$) in (F). Unpaired *t*-test. ns, no significance, **** $P < 0.0001$.

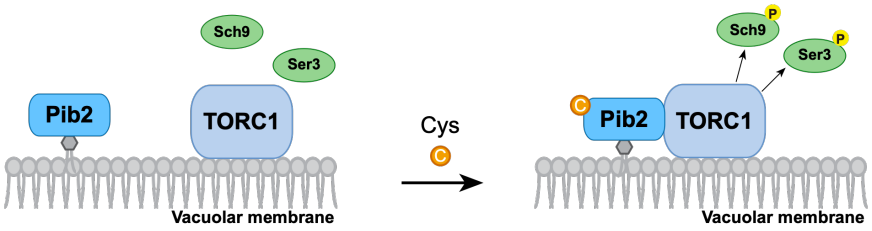

Figure 14. A model of Pib2-sensing cysteine activation of TORC1
The model shows how Pib2 senses cysteine to control TORC1 activity.

3. Discussion

In this study, I proposed that Pib2 serves as a cysteine sensor that contributes to TORC1 regulation in the yeast *S. cerevisiae*.

Cysteine was previously shown to activate TORC1 *in vitro*[53,65]. Here I revealed that cysteine was the most effective activator of the Pib2-dependent pathway. Further, I showed that cysteine binds to Pib2 via the T motif, and determined that the two most critical residues for this binding are W632 and F635. The T motif has been reported to be essential for the Pib2 activation of TORC1[51,52]. Cysteine-Pib2 binding enhances TORC1 binding via the E domain (residues 304-425); it was previously shown that this domain is the Kog1-binding domain of Pib2 and that it engages in Pib2-TORC1 interaction (Figure 14)[52,54,65]. D-cysteine, the enantiomer of L-cysteine, did not promote Pib2-TORC1 interaction. Further, TORC1 activation by the other Pib2-binding amino acid, glutamine, was not affected by the loss of the two critical residues W632 and F635, indicating that the structural properties of L-cysteine are crucial for this binding. Although intracellular cysteine concentrations vary depending on numerous factors, such as genetic background and growth conditions, some studies reported concentrations of approximately 80 μM[85,86]. My results indicated that TORC1 was minimally activated by adding 50-100 μM cysteine to the medium, and the dissociation constant of Pib2 for cysteine was determined to be 136.5 μM. Pib2 sways due to its intrinsically disordered regions (IDRs), and this movement promotes the dissociation of glutamine[65], which might influence cysteine

binding. Additional structural studies will provide insight into which properties of cysteine-Pib2 binding enhance the interaction of Pib2 with TORC1.

Cysteine has many metabolic and regulatory roles in yeast cells, not only through its function as a proteinogenic amino acid, but also as a precursor for pivotal molecules such as glutathione, taurine, coenzyme A, and iron-sulfur clusters, all of which play crucial roles in numerous cellular reactions[87–89]. Therefore, it is reasonable that cysteine levels are monitored by TORC1 activation in response to cellular demands.

Although there are some reports that the absence of either the Pib2 or Gtr pathway prevents Phase 1 (acute and transient) TORC1 activation by amino acids[52,92], my results suggest that different amino acids exhibit different dependencies on the Gtr and Pib2 pathways in the activation of TORC1. Consistent with previous reports, my results indicate that TORC1 activation by leucine[42,63] and methionine[64] is more dependent on the Gtr pathway, while activation by glutamine is more dependent on the Pib2 pathway[53,54]. I could not establish a general rule for the classification of amino acids into each type, even based on their relationship to metabolic pathways. Of note, however, the molecular weights of most Type 2 amino acids (Cys (121.2), Gly (75.07), Gln (146.1), Val (117.1) and Ala (89.09)) are smaller than those of Type 1 amino acids (Met (149.2), Leu (131.2), Ile (131.2), Glu (147.1), Asp (133.1), His (155.2), Phe (165.2), Tyr (181.2), and Trp (204.2)), which may help clarify this issue in the future.

An important observation is that Type 3 amino acids (Lys, Pro, and Arg) were

dependent on both the Gtr and Pib2 pathways. Multiple groups, including ours, have proposed that the Gtr pathway and Pib2 pathways act in parallel[51,53,54]. However, several reports have suggested a cooperative relationship between the two pathway[52,92]. Lys and Arg are both basic amino acids, which pool abundantly in vacuoles under nutrient-rich conditions and are released into the cytosol during nitrogen starvation[93]. Proline is the sole imino acid categorized as one of the poor amino acids as nitrogen source poorly supporting cellular growth[94]. It is unclear how these properties fit with my results; however, some sort of functional interaction between the two pathways may exist, at least in response to these amino acids.

Dr. Araki of our group has identified Ser3 as a novel substrate of TORC1. In addition to well-studied TORC1 substrates such as Sch9, Atg13, Sit4, Sfp1, Gln3, Ypk3[27,29–32,68], phosphoproteomic studies revealed several other possible TORC1 substrate[95], but Ser3 was not among them. Ser3 and Ser33 (behaves similar to Ser3) are phosphoglycerate dehydrogenases that are involved in serine biosynthesis[96]. We are now investigating the physiological significance of their phosphorylation, especially in terms of the activity of their enzymes, by analyzing their TORC1-dependent phosphorylation sites in another line of study. In this study, Ser3 expression is increased in *gtr1*Δ or *pib2*Δ cells. Meanwhile, in another study, I found that inactivated TORC1 increased the mRNA level of Ser3, but the mRNA level of Ser33 had no significant change. I also demonstrated that TORC1 represses SER3 expression by inducing long non-coding RNA SRG1 transcriptional interference, upon serine sufficiency. This implies that TORC1 acts as an

important regulator by sensing amino acid levels and thus regulating cellular metabolism.

Ser3 phosphorylation is not dependent on Gtr, but is instead wholly dependent on Pib2, indicating that Ser3 is Pib2 pathway-specific TORC1 substrate. It is an emerging concept that the phosphorylation of each (m)TORC1 substrate does not necessarily represent general activity status. For example, TFEB reacts differently than S6K and 4E-BP1 in response to specific inputs such as amino acids and growth factor[97]. This diversity stems from the different mechanisms whereby these substrates are recruited to mTORC1 via RagC. In mammals and *Schizosaccharomyces pombe*, some TORC1 substrates contain the TOS motif, by which they are recruited to TORC1 via binding to Raptor . Meanwhile, the distinct spatial distribution of TORC1 exhibits a diverse mechanism of substrate recruitment. In mammals, mTORC1 receives signals from lysosomes or the Golgi compartment, and the signals preferentially control S6K or 4E-BP, respectively[97]. In yeast, the differential localization of TORC1 on vacuoles or endosomes controls the phosphorylation of Sch9 or Atg13/Vps27[98]. However, Ser3 is the first identified substrate that is totally dependent on only one TORC1 pathway. Especially in *gtr1*Δ cells, Ser3 is colocalized with TROC1 in vacuole associated puncta, suggesting a physical association with TORC1 and/or Pib2. Elucidating the recruitment mechanism will help identify why Ser3 depends on the Pib2 pathway.

In conclusion, Pib2 serves as a cysteine sensor for the TORC1 pathway. This study expanded the concept that each amino acid is monitored individually in various

organisms in diverse manner. Cysteine activates mTORC1 in MEF cells in a manner dependent on Rag GTPase[51,99]. LAPF, a possible Pib2 homologue in humans, conserves the FYVE domain of Pib2 but does not affect glutamine-induced mTORC1 activation[99]. However, LAPF conserves the T motif of Pib2, including two crucial amino acid residues, W632 and F635[51], In the future it will be interesting to explore LAPF function in the context of mammalian cysteine sensing and metabolic regulation.

4. Materials and Methods

4.1 Key resources table

REAGENT or RESOURCE	SOURCE	IDENTIFIER
Antibodies		
Mouse monoclonal anti-PGK1 antibody	Thermo Fisher	459250; RRID: AB_2532235
Mouse monoclonal anti-GFP antibody	Roche	11814460001; RRID:AB_390913
Goat polyclonal anti-Tor1 (yN-15) antibody	Santa Cruz	sc-11900; RRID: AB_672897
Rat monoclonal anti-HA antibody	Roche	11867423001; RRID:AB_390918
anti-Sch9 antibody	Lab stock	N/A
anti-phospho-Sch9-T737 antibody	Lab stock	N/A
anti-Pib2 antibody	Lab stock	N/A
anti-GST antibody	Lab stock	N/A
HRP-conjugated goat anti-mouse IgG antibody	Jackson ImmunoResearch	115-035-003; RRID:AB_10015289
HRP-conjugated goat anti-rabbit IgG antibody	Jackson ImmunoResearch	111-035-003; RRID:AB_2313567
HRP-conjugated goat anti-rat IgG antibody	Cell Signaling Technology	7077; RRID:AB_10694715
HRP-conjugated rabbit anti-goat IgG antibody (anti-TAP)	Abcam	ab6741; RRID:AB_955424
Bacterial and virus strains		
E. coli DH5α	BioElegen Technology	DH01-20

E. coli Rosetta 2 (DE3)	Novagen	71397
Chemicals, peptide and recombinant proteins		
Cycloheximide	Nacalai tesque	66-81-9
Rapamycin	LKT Laboratories	53123-88-9
Yeast extract	BD Biosciences	212750
Peptone	BD Biosciences	211677
Glucose	Wako	50-99-7
Yeast nitrogen base without amino acids and ammonium sulfate	BD Biosciences	DF0335-15-9
Ammonium sulfate	Nacalai tesque	7783-20-2
Casamino acid	BD Biosciences	223050
Trichloroacetic acid	Wako	76-03-9
Triton X-100	Wako	9002-93-1
Ethanol	Nacalai tesque	64-17-5
Urea	Wako	57-13-6
SDS	Nacalai tesque	151-21-3
EDTA	Sigma-Aldrich	60-00-4
Tris	Nacalai tesque	77-86-1
NaCl	Wako	7647-14-5
DTT	Wako	3483-12-3
PMSF	Wako	329-98-6
Complete EDTA-free protease inhibitor cocktail	Roche	11873580001
GST-Accept	Nacalai tesque	09277-56
IPTG (Isopropyl-β-D-thiogalactoside)	TAKARA	9030
DMSO	Sigma-Aldrich	67-68-5

Sodium phosphate	Wako	7558-79-4
Bromophenol blue	Sigma-Aldrich	115-39-9
IgG coupled to Dynabeads (M-270 Epoxy)	Thermo Fisher	14301
ChromoTek GFP-Trap Magnetic Agarose	Proteintech	gtma-100; RRID:AB_2631358
Chloramphenicol	Wako	56-75-7
Glutathione Sepharose beads	Nacalai tesque	09277-56
Reduced glutathione	Wako	70-18-8
L-[^{35}S]-Cysteine	PerkinElmer	NEG022T
Scintillation fluid	Nacalai tesque	09135-51
Coomassie brilliant blue	Wako	6104-59-2
L-Glycine	Wako	56-40-6
L-Alanine	Sigma-Aldrich	56-41-7
L-Serine	Sigma-Aldrich	56-45-1
L-Proline	Wako	147-85-3
L-Valine	Wako	72-18-4
L-Threonine	Sigma-Aldrich	72-19-5
L-Cysteine	Wako	52-90-4
L-Leucine	Sigma-Aldrich	61-90-5
L-Isoleucine	Sigma-Aldrich	73-32-5
L-Aspartate	Sigma-Aldrich	56-84-8
L-Glutamine	Wako	56-85-9
L-Lysine	Sigma-Aldrich	657-27-2
L-Glutamate	Sigma-Aldrich	142-49-2
L-Methionine	Wako	63-68-3

L-Histidine	Sigma-Aldrich	71-00-1
L-Phenylalanine	Sigma-Aldrich	63-91-2
L-Arginine	Wako	74-79-3
L-Tyrosine	Sigma-Aldrich	60-18-4
L-Tryptophan	Sigma-Aldrich	73-22-3
D-cysteine	Combi-Blocks	32443-99-5
myo-Inositol	Nacalai tesque	87-89-8
p-Aminobenzoic acid	Nacalai tesque	150-13-0
Uracil	Wako	66-22-8
Critical commercial assays		
Chemi-Lumi One Ultra	Nacalai tesque	11644-40
KOD One PCR Master Mix	TOYOBO	KMM-101
Protein Assay BCA kit	Nacalai tesque	06385-00
Experimental models: Organisms/strains		
BY4741	Brachmann et al., 1998[100]	*MAT***a** *his3Δ1 leu2Δ0 met15Δ0 ura3Δ0*
BY4742	Brachmann et al., 1998[100]	*MAT*α *his3Δ1 leu2Δ0 lys2Δ0 ura3Δ0*
YAY2864	This study	[BY4741] *SER3-3HA-kanMX4 pHLUM*
YAY2867	This study	[BY4741] *SER3-3HA-kanMX4 pHLUM gtr1Δ::hphNT1*
YAY2868	This study	[BY4741] *SER3-3HA-kanMX4 pHLUM pib2Δ::natNT2*
ZQZ108	This study	[BY4741] *gtr1Δ::natNT2 ego1Δ::zeoNT3 pHLUM*

ZQZ109	This study and Ukai et al., 2018[54]	[BY4741] *gtr1Δ::natNT2 ego1Δ::zeoNT3 pHLUM pib2-2-kanMX4*
ZQZ101	This study	[BY4741] *GFP-TOR1-LEU2 VPH1-mcherry-hphNT1 pHLUM*
ZQZ102	This study	[BY4741] *GFP-TOR1-LEU2 VPH1-mCherry-hphNT1 pHLUM gtr1Δ::natNT2*
ZQZ103	This study	[BY4741] *GFP-TOR1-LEU2 VPH1-mCherry-hphNT1 pHLUM pib2Δ::natNT2*
ZQZ148	This study	[BY4741] *VPH1-mCherry-hphNT1 ATG2-yeGFP-kanMX4*
ZQZ150	This study	[BY4741] *VPH1-mCherry-hphNT1 ATG2-yeGFP-kanMX4 gtr1Δ::zeoNT3*
ZQZ152	This study	[BY4741] *VPH1-mCherry-hphNT1 ATG2-yeGFP-kanMX4 pib2Δ::natNT2*
ZQZ232	This study	[BY4741] *gap1Δ::kanMX6 pHLUM*
ZQZ233	This study	[BY4741] *yct1Δ::kanMX6 pHLUM*
ZQZ114	This study	[BY4741] *yeGFP-PIB2 gtr1Δ::natNT2 pHLUM*
ZQZ118	This study	[BY4741] *SER3-3HA-kanMX4 pHLUM gtr1Δ::hphNT1 gsh1Δ::zeoNT3*
ZQZ137	This study	[BY4741] *VPH1-mCherry-hphNT1 GAP1-yeGFP-kanMX4*
ZQZ138	This study	[BY4741] *VPH1-mCherry-hphNT1 GAP1-yeGFP-kanMX4 pib2Δ::natNT2*

ZQZ146	This study	[BY4741] *VPH1-mCherry-hphNT1 YCT1-yeGFP-kanMX4*
ZQZ147	This study	[BY4741] *VPH1-mCherry-hphNT1 YCT1-yeGFP-kanMX4 pib2Δ::natNT2*
ZQZ116	This study	[BY4741] *yeGFP-PIB2 GTR1-TAP::kanMX4 pHLUM*
YAY2569	Ukai et al., 2018[54]	[BY4741] *pib2Δ::zeoNT3 GFP-PIB2^{full}-kanMX4*
YAY2575	Ukai et al., 2018[54]	[BY4741] *pib2Δ::zeoNT3 GFP-PIB2$^{50-635}$-kanMX4*
YAY2570	Ukai et al., 2018[54]	[BY4741] *pib2Δ::zeoNT3 GFP-PIB2$^{102-635}$-kanMX4*
YAY2571	Ukai et al., 2018[54]	[BY4741] *pib2Δ::zeoNT3 GFP-PIB2$^{165-635}$-kanMX4*
YAY2572	Ukai et al., 2018[54]	[BY4741] *pib2Δ::zeoNT3 GFP-PIB2$^{304-635}$-kanMX4*
YAY2573	Ukai et al., 2018[54]	[BY4741] *pib2Δ::zeoNT3 GFP-PIB2$^{440-635}$-kanMX4*
YAY2574	Ukai et al., 2018[54]	[BY4741] *pib2Δ::zeoNT3 GFP-PIB2$^{1-620}$-kanMX4*
ZQZ230	This study	[BY4741] *TAP-TOR1-LEU2 pib2Δ::natNT2*
ZQZ231	This study	[BY4741] *pACT1-TAP-NAT-leu2d0-int pib2Δ::natNT2*
HUY28A	This study	[BY4741] *pib2Δ::zeoNT3*
ZQZ238	This study	[BY4741] *pib2Δ::zeoNT3 GFP-PIB2$^{S621A\ V622A\ I623A}$-kanMX4*
ZQZ239	This study	[BY4741] *pib2Δ::zeoNT3 GFP-PIB2$^{G624A\ S625A\ V626A}$-kanMX4*

ZQZ240	This study	[BY4741] *pib2Δ::zeoNT3 GFP-PIB2$^{P627A\ A628D\ N629A}$-kanMX4*
ZQZ241	This study	[BY4741] *pib2Δ::zeoNT3 GFP-PIB2$^{W630A\ N631A\ W632A}$-kanMX4*
ZQZ242	This study	[BY4741] *pib2Δ::zeoNT3 GFP-PIB2$^{S633A\ S634A\ F635A}$-kanMX4*
ZQZ253	This study	[BY4741] *pib2Δ::zeoNT3 GFP-PIB2^{W630A}-kanMX4*
ZQZ254	This study	[BY4741] *pib2Δ::zeoNT3 GFP-PIB2 ^{N631A}-kanMX4*
ZQZ255	This study	[BY4741] *pib2Δ::zeoNT3 GFP-PIB2^{W632A}-kanMX4*
ZQZ256	This study	[BY4741] *pib2Δ::zeoNT3 GFP-PIB2^{S633A}-kanMX4*
ZQZ257	This study	[BY4741] *pib2Δ::zeoNT3 GFP-PIB2^{S634A}-kanMX4*
ZQZ258	This study	[BY4741] *pib2Δ::zeoNT3 GFP-PIB2^{F635A}-kanMX4*
ZQZ264	This study	[BY4741] *pib2Δ::zeoNT3 PIB2^{W632A}-kanMX4*
ZQZ265	This study	[BY4741] *pib2Δ::zeoNT3 PIB2^{F635A}-kanMX4*
Recombinant DNA		
pHLUM	Mülleder et al., 2012[77]	*LEU2*, *URA3*, *HIS3*, *MET15/17*
pYA1112	This study	*pACT1-TAP-NAT-leu2d0-int*
pYA1340	This study	*pET28a-SER3*
pGEX-6P1-PIB2$^{304-635}$	This study	[pGEX-6P-1(+)] *GST-PIB2$^{304-635}$*
pGEX-6P1-PIB2$^{440-635}$	This study	[pGEX-6P-1(+)] *GST-PIB2$^{440-635}$*
pGEX-6P1-PIB2$^{304-620}$	This study	[pGEX-6P-1(+)] *GST-PIB2$^{304-620}$*

pGEX-6P1-PIB2$^{304\text{-}635\ (W632A)}$	This study	[pGEX-6P-1(+)] *GST-PIB2$^{304\text{-}635\ (W632A)}$*
pGEX-6P1-PIB2$^{304\text{-}635\ (F635A)}$	This study	[pGEX-6P-1(+)] *GST-PIB2$^{304\text{-}635\ (F635A)}$*
pRS316	Sikorski and Hieter, 1989[101]	CEN, *URA3*
pSK114	Kira et al., 2016[72]	[pRS316] *GTR1*
Software and algorithms		
ImageJ	NIH	https://imagej.nih.gov/ij/
Photoshop	Adobe	https://www.adobe.com
Jalview	Waterhouse et al., 2009[102]	https://www.jalview.org/
Graphic	Picta Inc	https://www.graphic.com/
GraphPad Prism	GraphPad Software	https://www.graphpad.com/

4.2 Experimental model and subject details

S. cerevisiae strains are listed in the Key Resources Table. They were grown as described in the Method Details. Recombinant proteins, including GST-PIB2$^{304\text{-}635}$, GST-PIB2$^{440\text{-}635}$, GST-PIB2$^{304\text{-}620}$, GST-PIB2$^{304\text{-}635\ (W632A)}$, and GST-PIB2$^{304\text{-}635\ (F635A)}$, were expressed in *E. coli* Rosetta 2 (DE3), and cloning procedures were conducted in *E. coli* DH5α.

4.3 Yeast strains, plasmid, and growth conditions

S. cerevisiae strains and plasmids used in this study are listed in the Key Resources Table. Strain construction, gene deletion, and chromosomal epitope tagging were performed as previously reported[103,104]. Plasmids amplifications were performed using *E. coli* DH5α, and plasmids sequences were verified by Sanger sequencing (GeneWiz). Yeast cells were grown to mid-log phase in YPD medium (1% yeast extract, 2% peptone, and 2% glucose), SCD medium (0.17% yeast nitrogen base without amino acids and ammonium sulfate, 0.5% ammonium sulfate, 0.5% casamino acid, 2% glucose), SD-N medium (0.17% yeast nitrogen base without amino acids and ammonium sulfate, 2% glucose), or SD-N medium with complete amino acids (0.17% yeast nitrogen base without amino acids and ammonium sulfate, 2% glucose, 0.2% drop-out mix). Unless otherwise indicated, yeast cells were cultured at 30 °C. Rapamycin was added to medium at a final concentration of 0.2 μg/ml using a stock solution (1 mg/ml in ethanol and Triton X-100 at a ratio of 9:1 (v/v)). Cycloheximide was added to the medium at a final concentration of 25 μg/ml using a stock solution (50mg/ml in DMSO). Each amino acid was added to medium as 5 mM from 50 times stock solution otherwise indicated. Detailed composition of drop-out mix is as follows: 0.5 g of adenine, 2 g of alanine, 2 g of arginine, 2g of asparagine, 2 g of aspartic acid, 2 g of cysteine, 2 g of glutamine, 2 g of glutamic acid, 2 g of glycine, 2 g of histidine, 2 g of myo-inositol, 2 g of isoleucine, 10 g of leucine, 2 g of lysine, 2 g of methionine, 0.2 g

of p-aminobenzoic acid, 2 g of phenylalanine, 2 g of proline, 2 g of serine, 2 g of threonine, 2 g of tryptophan, 2 g of tyrosine, 2 g of uracil, 2 g of valine.

4.4 Cell lysates preparation and western blot analyses

Cells lysates were prepared as previously reported with slight modifications[27]. Briefly, 2 OD_{600} units of cells were harvested and treated with 10% trichloroacetic acid for at least 15 min on ice. The precipitated protein was pelleted by centrifugation at 20,000 × *g* for 15 min at 4 °C. The pellets were re-dissolved in 50 µl of high urea buffer (HU buffer: 8 M urea, 5% SDS, 1 mM EDTA, 200 mM sodium phosphate (pH 6.8), 100 mM DTT, traces of bromophenol blue). Cells were lysed using a FastPrep instrument (MP-Biomedicals) with 0.5-mm zirconia beads for three cycles (speed 5.0 for 20 s), followed by heating for 15 min at 65 °C and vortexing for 2 min. The cell lysates were centrifuged at 20,000 × *g* for 5 min and subjected to SDS-PAGE and western blot analysis using the indicated antibodies.

4.5 Fluorescence microscopy

Cells were grown in SCD medium and then shifted to SD-N medium for 30 min of nitrogen starvation, and the indicated amino acids were added. Cells were collected by centrifugation (600 × *g*, 2 min) and subjected to microscopy. Cells were observed using a Leica AF6500 fluorescence imaging system (Leica Microsystems) mounted on a

DMI6000B microscope (HCX PL APO 100/1.40-0.70 oil-immersion objective lens, xenon lamp (Leica Microsystems)) under the control of LAS-AF software (Leica Microsystems). ImageJ software was used to process images.

4.6 Immunoprecipitation experiments

Cells were resuspended in TAP-A buffer (50 mM Tris-HCl (pH 8.0), 150 mM NaCl, 10% glycerol, 1 mM DTT, 1 mM PMSF, 1 μM microcystin-LR, PhosSTOP, and 1 mM EDTA supplemented with Complete EDTA-free protease inhibitor cocktail) and lysed with a FastPrep instrument (MP-Biomedicals) and 0.5-mm zirconia beads. After lysis, cell lysates were incubated with Triton X-100 (0.2% final concentration) for 10 min at 4 °C, and then clarified by centrifugation at 20,000 × *g* for 10 min at 4 °C. Gtr1-TAP or TAP-Tor1 proteins were precipitated with magnetic beads covalently coupled to rabbit IgG (Dynabeads M-270 Epoxy beads: Invitrogen) at 4 °C. GFP-Pib2 proteins were precipitated with magnetic GFP-Trap-M beads (Chromotek) at 4 °C. The beads were washed three times with TAP-A buffer containing 0.2% Triton X-100. If indicated, all immunoprecipitation buffers were added with the specified final concentration of L-cysteine, D-cysteine, L-leucine, or L-methionine. If indicated, L-cysteine was added to the immunoprecipitation buffers at a final concentration of 30 mM. Bound proteins were eluted from beads by heating for 15 min at 65 °C in high-urea buffer, then subjected to SDS-PAGE and western blot analysis.

Quantitative analyses of the blots were performed using ImageJ software when necessary.

4.7 Protein purification

E. coli Rosetta 2 (DE3) carrying pGEX-6P-1(+)-derived plasmids were grown in LB medium containing 50 μg mL^{-1} ampicillin and 25 μg mL^{-1} chloramphenicol at 37 °C overnight. The bacterial culture was diluted to an OD_{600} of 0.1 in LB medium containing 50 μg mL^{-1} ampicillin and 25 μg mL^{-1} chloramphenicol, and then cultured to an OD_{600} of 0.7 at 37 °C. The bacterial culture was incubated on ice for 30 min before the addition of IPTG. Expression was induced by 0.25 mM IPTG at 23 °C for 6 h. Cells were collected, suspended in lysis buffer (50 mM Tris-HCl (pH 8.0), 150 mM NaCl, 10% glycerol, 1 mM DTT, 1 mM PMSF, and 1 mM EDTA supplemented with Complete EDTA-free protease inhibitor cocktail), and lysed by sonication (AmpI: 40%; 0.7 s on/0.3 s off; 30 cycles). Then lysates were incubated with Triton X-100 (0.2% final concentration) for 10 min at 4 °C and clarified by centrifugation at 20,000 × *g* for 10 min at 4 °C. The GST-tagged proteins were incubated with glutathione Sepharose beads for 2 h at 4 °C, washed with TAP-B buffer (50 mM Tris-HCl (pH 8.0), 150 mM NaCl, 10% glycerol, 1 mM EDTA, 1 mM DTT), and eluted with elution buffer (50 mM Tris-HCl (pH 8.0), 150 mM NaCl, 10% glycerol, 1 mM EDTA, 1 mM DTT, 20 mM reduced glutathione). Proteins immobilized on the beads were eluted with Laemmli buffer by heating for 5 min at 95 °C. Protein

samples were resolved by SDS-PAGE and CBB staining.

4.8 *In vitro* binding assay

To examine the Pib2-Tor1 interaction in response to changes in cysteine levels, TAP-Tor1 was purified from TAP-Tor1 expressing yeast as described above. GST-tagged Pib2(304-635) was purified from *E. coli* Rosetta 2 (DE3) as described above. Then purified TAP-Tor1 on magnetic beads was suspended in pull-down buffer (50 mM Tris-HCl (pH 8.0), 150 mM NaCl, 10% glycerol, 1 mM EDTA, 1 mM DTT), mixed with GST-Pib2(304-635) along with the indicated concentration of L-cysteine, D-cysteine or L-methionine, and then rotated at 4 °C for 3 h. Following this, the magnetic beads were washed three times with pull-down buffer, suspended in HU buffer, and heated at 65 °C for 15 min. Proteins were separated using SDS-PAGE and analyzed by immunoblotting.

4.9 Cysteine uptake assay

Radiolabeled amino acid uptake was performed as previously reported with slight modifications[82,83,105]. Briefly, cells were grown in SCD medium until mid-log phase, followed by nitrogen starvation using SD-N medium for 30 min. Cells were harvested and suspended in 300 µl SD-N medium. The assay medium contained 0.35 µCi L-[^{35}S]-cysteine in SD-N medium and a final concentration of 0.25 mM of cysteine, and was warmed to 30 °C. The cysteine uptake assay was initiated by the addition of 100 µl of

pre-warmed cell suspension to 100 µl of assay medium and then incubated for 5 min at 30 °C. The uptake assay was stopped by adding 1 ml SD-N medium with 25 mM L-cysteine. The cells were collected on a glass-fiber filter (Cytiva, 1827-025) by aspiration and washed three times with SD-N medium with 0.25 mM L-cysteine. The filter was immersed in 3 ml of scintillation fluid and radioactivity was measured using a liquid scintillation counter (Tri-Carb 2810 TR, PerkinElmer). Background activity was determined by following the same procedure as in the experimental group described above, but without adding any cells. The amount of accumulated compound was calculated as previously reported[105].

4.10 Cysteine-binding assay and K_d calculation

Amino acids binding assays performed as previously reported[73]. GST-Pib2(304-635), GST-Pib2(440-635), GST-Pib2(304-620), GST-Pib2(304-635), GST-Pib2(304-635) mutant (W632A) and GST-Pib2(304-635) mutant (F635A) proteins were expressed in *E. coli* Rosetta 2 (DE3) by inducing 0.25 mM IPTG for 6 h at 23 °C. Following purification of the GST-tagged protein, the Glutathione Sepharose beads were washed four times with TAP-B buffer (50 mM Tris-HCl (pH 8.0), 150 mM NaCl, 10% glycerol, 1 mM EDTA, 1 mM DTT), and a portion of the purified protein was analyzed by SDS-PAGE and Coomassie brilliant blue (CBB) staining. The beads were suspended in 200 µl TAP-B buffer and incubated for 3 h on ice with the indicated amount of L-[^{35}S]-cysteine

and unlabeled cysteine. After incubation, the beads were washed four times with TAP-B buffer, resuspended in 900 µl TAP-B buffer, and then 300 µl aliquots were separately added to 3 ml scintillation fluid. The radioactivity was measured using a liquid scintillation counter (Tri-Carb 2810 TR, PerkinElmer). The affinity of Pib2 for cysteine was determined as previously reported[73].

4.11 LC-MS analysis

Cells expressing GFP-Pib2 were grown in SCD medium until mid-log phase, followed by nitrogen starvation using SD-N medium for 30 min, and then restimulated with or without 5 mM cysteine for 15 min. GFP-Pib2 was immunoprecipitated as previously descried. GFP-Pib2 was eluted from beads by heating for 15 min at 65°C in HU buffer, then subjected to SDS-PAGE and CBB staining. The subsequent sample preparation and LC-MS assay were performed by the CoMIT Omics Center of the Graduate School of Medicine at Osaka University. The abundance of each protein was quantified using the exponentially modified Protein Abundance Index (emPAI), which estimates the absolute protein abundance based on the number of peptides identified by MS[106].

5. References

1. Vézina, C., Kudelski, A., and Sehgal, S.N. (1975). Rapamycin (AY-22,989), a new antifungal antibiotic. I. Taxonomy of the producing streptomycete and isolation of the active principle. J. Antibiot. (Tokyo) *28*, 721–726. 10.7164/antibiotics.28.721.
2. Douros, J., and Suffness, M. (1981). New antitumor substances of natural origin. Cancer Treat. Rev. *8*, 63–87. 10.1016/S0305-7372(81)80006-0.
3. Martel, R.R., Klicius, J., and Galet, S. (1977). Inhibition of the immune response by rapamycin, a new antifungal antibiotic. Can. J. Physiol. Pharmacol. *55*, 48–51. 10.1139/y77-007.
4. Rosen, M., Standaert, R., Galat, A., Nakatsuka, M., and Schreiber, S. (1990). Inhibition of FKBP Rotamase Activity by Immunosuppressant FK506: Twisted Amide Surrogate. Science *248*, 863–866. 10.1126/science.1693013.
5. Standaert, R.F., Galat, A., Verdine, G.L., and Schreiber, S.L. (1990). Molecular cloning and overexpression of the human FKS06-binding protein FKBP. Nature *346*, 671–674. 10.1038/346671a0.
6. Heitman, J., Movva, N.R., and Hall, M.N. (1991). Targets for cell cycle arrest by the immunosuppressant rapamycin in yeast. Science *253*, 905–909. 10.1126/science.1715094.
7. Chen, J., Zheng, X.F., Brown, E.J., and Schreiber, S.L. (1995). Identification of an 11-kDa FKBP12-rapamycin-binding domain within the 289-kDa FKBP12-

rapamycin-associated protein and characterization of a critical serine residue. Proc. Natl. Acad. Sci. *92*, 4947–4951. 10.1073/pnas.92.11.4947.

8. Sabatini, D.M., Erdjument-Bromage, H., Lui, M., Tempst, P., and Snyder, S.H. (1994). RAFT1: A mammalian protein that binds to FKBP12 in a rapamycin-dependent fashion and is homologous to yeast TORs. Cell *78*, 35–43. 10.1016/0092-8674(94)90570-3.
9. Sabers, C.J., Martin, M.M., Brunn, G.J., Williams, J.M., Dumont, F.J., Wiederrecht, G., and Abraham, R.T. (1995). Isolation of a Protein Target of the FKBP12-Rapamycin Complex in Mammalian Cells (∗). J. Biol. Chem. *270*, 815–822. 10.1074/jbc.270.2.815.
10. Noda, T., and Ohsumi, Y. (1998). Tor, a phosphatidylinositol kinase homologue, controls autophagy in yeast. J. Biol. Chem. *273*, 3963–3966. 10.1074/jbc.273.7.3963.
11. Jacinto, E., Loewith, R., Schmidt, A., Lin, S., Rüegg, M.A., Hall, A., and Hall, M.N. (2004). Mammalian TOR complex 2 controls the actin cytoskeleton and is rapamycin insensitive. Nat. Cell Biol. *6*, 1122–1128. 10.1038/ncb1183.
12. Loewith, R., Jacinto, E., Wullschleger, S., Lorberg, A., Crespo, J.L., Bonenfant, D., Oppliger, W., Jenoe, P., and Hall, M.N. (2002). Two TOR Complexes, Only One of which Is Rapamycin Sensitive, Have Distinct Roles in Cell Growth Control. Mol. Cell *10*, 457–468. 10.1016/S1097-2765(02)00636-6.
13. Sarbassov, Ali, S.M., Kim, D.-H., Guertin, D.A., Latek, R.R., Erdjument-Bromage, H., Tempst, P., and Sabatini, D.M. (2004). Rictor, a Novel Binding Partner of

mTOR, Defines a Rapamycin-Insensitive and Raptor-Independent Pathway that Regulates the Cytoskeleton. Curr. Biol. *14*, 1296–1302. 10.1016/j.cub.2004.06.054.

14. Hara, K., Maruki, Y., Long, X., Yoshino, K., Oshiro, N., Hidayat, S., Tokunaga, C., Avruch, J., and Yonezawa, K. (2002). Raptor, a Binding Partner of Target of Rapamycin (TOR), Mediates TOR Action. Cell *110*, 177–189. 10.1016/S0092-8674(02)00833-4.

15. Kim, D.-H., Sarbassov, D.D., Ali, S.M., Latek, R.R., Guntur, K.V.P., Erdjument-Bromage, H., Tempst, P., and Sabatini, D.M. (2003). GβL, a Positive Regulator of the Rapamycin-Sensitive Pathway Required for the Nutrient-Sensitive Interaction between Raptor and mTOR. Mol. Cell *11*, 895–904. 10.1016/S1097-2765(03)00114-X.

16. Kim, D.-H., Sarbassov, D.D., Ali, S.M., King, J.E., Latek, R.R., Erdjument-Bromage, H., Tempst, P., and Sabatini, D.M. (2002). mTOR Interacts with Raptor to Form a Nutrient-Sensitive Complex that Signals to the Cell Growth Machinery. Cell *110*, 163–175. 10.1016/S0092-8674(02)00808-5.

17. Peterson, T.R., Laplante, M., Thoreen, C.C., Sancak, Y., Kang, S.A., Kuehl, W.M., Gray, N.S., and Sabatini, D.M. (2009). DEPTOR Is an mTOR Inhibitor Frequently Overexpressed in Multiple Myeloma Cells and Required for Their Survival. Cell *137*, 873–886. 10.1016/j.cell.2009.03.046.

18. Wang, L., Harris, T.E., Roth, R.A., and Lawrence, J.C. (2007). PRAS40 Regulates mTORC1 Kinase Activity by Functioning as a Direct Inhibitor of Substrate Binding.

J. Biol. Chem. *282*, 20036–20044. 10.1074/jbc.M702376200.

19. Frias, M.A., Thoreen, C.C., Jaffe, J.D., Schroder, W., Sculley, T., Carr, S.A., and Sabatini, D.M. (2006). mSin1 Is Necessary for Akt/PKB Phosphorylation, and Its Isoforms Define Three Distinct mTORC2s. Curr. Biol. *16*, 1865–1870. 10.1016/j.cub.2006.08.001.

20. Jacinto, E., Facchinetti, V., Liu, D., Soto, N., Wei, S., Jung, S.Y., Huang, Q., Qin, J., and Su, B. (2006). SIN1/MIP1 Maintains rictor-mTOR Complex Integrity and Regulates Akt Phosphorylation and Substrate Specificity. Cell *127*, 125–137. 10.1016/j.cell.2006.08.033.

21. Woo, S.-Y., Kim, D.-H., Jun, C.-B., Kim, Y.-M., Haar, E.V., Lee, S., Hegg, J.W., Bandhakavi, S., Griffin, T.J., and Kim, D.-H. (2007). PRR5, a Novel Component of mTOR Complex 2, Regulates Platelet-derived Growth Factor Receptor β Expression and Signaling. J. Biol. Chem. *282*, 25604–25612. 10.1074/jbc.M704343200.

22. Yang, Q., Inoki, K., Ikenoue, T., and Guan, K.-L. (2006). Identification of Sin1 as an essential TORC2 component required for complex formation and kinase activity. Genes Dev. *20*, 2820–2832. 10.1101/gad.1461206.

23. Reinke, A., Anderson, S., McCaffery, J.M., Yates, J., Aronova, S., Chu, S., Fairclough, S., Iverson, C., Wedaman, K.P., and Powers, T. (2004). TOR Complex 1 Includes a Novel Component, Tco89p (YPL180w), and Cooperates with Ssd1p to Maintain Cellular Integrity in Saccharomyces cerevisiae. J. Biol. Chem. *279*, 14752–14762. 10.1074/jbc.M313062200.

24. Wedaman, K.P., Reinke, A., Anderson, S., Yates, J., McCaffery, J.M., and Powers, T. (2003). Tor Kinases Are in Distinct Membrane-associated Protein Complexes in Saccharomyces cerevisiae. Mol. Biol. Cell *14*, 1204–1220. 10.1091/mbc.e02-09-0609.

25. Zinzalla, V., Sturgill, T.W., and Hall, M.N. (2010). Chapter 1 - TOR Complexes: Composition, Structure, and Phosphorylation. In The Enzymes The Enzymes. (Academic Press), pp. 1–20. 10.1016/S1874-6047(10)27001-4.

26. Loewith, R., and Hall, M.N. (2011). Target of rapamycin (TOR) in nutrient signaling and growth control. Genetics *189*, 1177–1201. 10.1534/genetics.111.133363.

27. Urban, J., Soulard, A., Huber, A., Lippman, S., Mukhopadhyay, D., Deloche, O., Wanke, V., Anrather, D., Ammerer, G., Riezman, H., et al. (2007). Sch9 is a major target of TORC1 in Saccharomyces cerevisiae. Mol. Cell *26*, 663–674. 10.1016/j.molcel.2007.04.020.

28. Noda, T. (2017). Regulation of Autophagy through TORC1 and mTORC1. Biomolecules *7*, 52. 10.3390/biom7030052.

29. Lempiäinen, H., Uotila, A., Urban, J., Dohnal, I., Ammerer, G., Loewith, R., and Shore, D. (2009). Sfp1 interaction with TORC1 and Mrs6 reveals feedback regulation on TOR signaling. Mol. Cell *33*, 704–716. 10.1016/j.molcel.2009.01.034.

30. Bertram, P.G., Choi, J.H., Carvalho, J., Ai, W., Zeng, C., Chan, T.-F., and Zheng, X.F.S. (2000). Tripartite Regulation of Gln3p by TOR, Ure2p, and Phosphatases. J.

Biol. Chem. *275*, 35727–35733. 10.1074/jbc.M004235200.

31. Boeckstaens, M., Llinares, E., Van Vooren, P., and Marini, A.M. (2014). The TORC1 effector kinase Npr1 fine tunes the inherent activity of the Mep2 ammonium transport protein. Nat. Commun. *5*, 3101. 10.1038/ncomms4101.

32. Yerlikaya, S., Meusburger, M., Kumari, R., Huber, A., Anrather, D., Costanzo, M., Boone, C., Ammerer, G., Baranov, P.V., and Loewith, R. (2016). TORC1 and TORC2 work together to regulate ribosomal protein S6 phosphorylation in *Saccharomyces cerevisiae*. Mol. Biol. Cell *27*, 397–409. 10.1091/mbc.e15-08-0594.

33. Inoki, K., Li, Y., Xu, T., and Guan, K.-L. (2003). Rheb GTPase is a direct target of TSC2 GAP activity and regulates mTOR signaling. Genes Dev. *17*, 1829–1834. 10.1101/gad.1110003.

34. Inoki, K., Li, Y., Zhu, T., Wu, J., and Guan, K.-L. (2002). TSC2 is phosphorylated and inhibited by Akt and suppresses mTOR signalling. Nat. Cell Biol. *4*, 648–657. 10.1038/ncb839.

35. Potter, C.J., Huang, H., and Xu, T. (2001). Drosophila Tsc1 Functions with Tsc2 to Antagonize Insulin Signaling in Regulating Cell Growth, Cell Proliferation, and Organ Size. Cell *105*, 357–368. 10.1016/S0092-8674(01)00333-6.

36. Hao, F., Kondo, K., Itoh, T., Ikari, S., Nada, S., Okada, M., and Noda, T. (2017). Rheb localized on the Golgi membrane activates lysosome-localized mTORC1 at the Golgi-lysosome contact site. J. Cell Sci., jcs.208017. 10.1242/jcs.208017.

37. Bar-Peled, L., Schweitzer, L.D., Zoncu, R., and Sabatini, D.M. (2012). Ragulator Is

a GEF for the Rag GTPases that Signal Amino Acid Levels to mTORC1. Cell *150*, 1196–1208. 10.1016/j.cell.2012.07.032.

38. Sancak, Y., Bar-Peled, L., Zoncu, R., Markhard, A.L., Nada, S., and Sabatini, D.M. (2010). Ragulator-Rag complex targets mTORC1 to the lysosomal surface and Is necessary for Its activation by amino acids. Cell *141*, 290–303. 10.1016/j.cell.2010.02.024.

39. Kim, E., Goraksha-Hicks, P., Li, L., Neufeld, T.P., and Guan, K.-L. (2008). Regulation of TORC1 by Rag GTPases in nutrient response. Nat. Cell Biol. *10*, 935–945. 10.1038/ncb1753.

40. Sancak, Y., Peterson, T.R., Shaul, Y.D., Lindquist, R.A., Thoreen, C.C., Bar-Peled, L., and Sabatini, D.M. (2008). The Rag GTPases bind raptor and mediate amino acid signaling to mTORC1. Science *320*, 1496–1501. 10.1126/science.1157535.

41. Jewell, J.L., Russell, R.C., and Guan, K.-L. (2013). Amino acid signalling upstream of mTOR. Nat. Rev. Mol. Cell Biol. *14*, 133–139. 10.1038/nrm3522.

42. Binda, M., Péli-Gulli, M.-P., Bonfils, G., Panchaud, N., Urban, J., Sturgill, T.W., Loewith, R., and De Virgilio, C. (2009). The Vam6 GEF controls TORC1 by activating the EGO Complex. Mol. Cell *35*, 563–573. 10.1016/j.molcel.2009.06.033.

43. Powis, K., Zhang, T., Panchaud, N., Wang, R., Virgilio, C.D., and Ding, J. (2015). Crystal structure of the Ego1-Ego2-Ego3 complex and its role in promoting Rag GTPase-dependent TORC1 signaling. Cell Res. *25*, 1043–1059. 10.1038/cr.2015.86.

44. Bar-Peled, L., Chantranupong, L., Cherniack, A.D., Chen, W.W., Ottina, K.A.,

Grabiner, B.C., Spear, E.D., Carter, S.L., Meyerson, M., and Sabatini, D.M. (2013). A Tumor suppressor complex with GAP activity for the Rag GTPases That signal amino acid sufficiency to mTORC1. Science *340*, 1100–1106. 10.1126/science.1232044.

45. Condon, K.J., and Sabatini, D.M. (2019). Nutrient regulation of mTORC1 at a glance. J. Cell Sci. *132*, jcs222570. 10.1242/jcs.222570.

46. Algret, R., Fernandez-Martinez, J., Shi, Y., Kim, S.J., Pellarin, R., Cimermancic, P., Cochet, E., Sali, A., Chait, B.T., Rout, M.P., et al. (2014). Molecular Architecture and Function of the SEA Complex, a Modulator of the TORC1 Pathway. Mol. Cell. Proteomics MCP *13*, 2855–2870. 10.1074/mcp.M114.039388.

47. Kira, S., Tabata, K., Shirahama-Noda, K., Nozoe, A., Yoshimori, T., and Noda, T. (2014). Reciprocal conversion of Gtr1 and Gtr2 nucleotide-binding states by Npr2-Npr3 inactivates TORC1 and induces autophagy. Autophagy *10*, 1565–1578. 10.4161/auto.29397.

48. Panchaud, N., Péli-Gulli, M.-P., and De Virgilio, C. (2013). SEACing the GAP that nEGOCiates TORC1 activation: Evolutionary conservation of Rag GTPase regulation. Cell Cycle *12*, 2948–2952. 10.4161/cc.26000.

49. Panchaud, N., Péli-Gulli, M.-P., and De Virgilio, C. (2013). Amino acid deprivation inhibits TORC1 through a GTPase-activating protein complex for the Rag family GTPase Gtr1. Sci. Signal. *6*. 10.1126/scisignal.2004112.

50. Nicastro, R., Sardu, A., Panchaud, N., and De Virgilio, C. (2017). The Architecture

of the Rag GTPase Signaling Network. Biomolecules *7*, 48. 10.3390/biom7030048.

51. Kim, A., and Cunningham, K.W. (2015). A LAPF/phafin1-like protein regulates TORC1 and lysosomal membrane permeabilization in response to endoplasmic reticulum membrane stress. Mol. Biol. Cell *26*, 4631–4645. 10.1091/mbc.E15-08-0581.

52. Michel, A.H., Hatakeyama, R., Kimmig, P., Arter, M., Peter, M., Matos, J., De Virgilio, C., and Kornmann, B. (2017). Functional mapping of yeast genomes by saturated transposition. eLife *6*, e23570. 10.7554/eLife.23570.

53. Tanigawa, M., and Maeda, T. (2017). An *In Vitro* TORC1 Kinase Assay That Recapitulates the Gtr-Independent Glutamine-Responsive TORC1 Activation Mechanism on Yeast Vacuoles. Mol. Cell. Biol. *37*, e00075-17. 10.1128/MCB.00075-17.

54. Ukai, H., Araki, Y., Kira, S., Oikawa, Y., May, A.I., and Noda, T. (2018). Gtr/Ego-independent TORC1 activation is achieved through a glutamine-sensitive interaction with Pib2 on the vacuolar membrane. PLOS Genet. *14*, e1007334. 10.1371/journal.pgen.1007334.

55. Chantranupong, L., Wolfson, R.L., Orozco, J.M., Saxton, R.A., Scaria, S.M., Bar-Peled, L., Spooner, E., Isasa, M., Gygi, S.P., and Sabatini, D.M. (2014). The Sestrins Interact with GATOR2 to Negatively Regulate the Amino-Acid-Sensing Pathway Upstream of mTORC1. Cell Rep. *9*, 1–8. 10.1016/j.celrep.2014.09.014.

56. Parmigiani, A., Nourbakhsh, A., Ding, B., Wang, W., Kim, Y.C., Akopiants, K.,

Guan, K.-L., Karin, M., and Budanov, A.V. (2014). Sestrins Inhibit mTORC1 Kinase Activation through the GATOR Complex. Cell Rep. *9*, 1281–1291. 10.1016/j.celrep.2014.10.019.

57. Saxton, R.A., Knockenhauer, K.E., Wolfson, R.L., Chantranupong, L., Pacold, M.E., Wang, T., Schwartz, T.U., and Sabatini, D.M. (2016). Structural basis for leucine sensing by the Sestrin2-mTORC1 pathway. Science *351*, 53–58. 10.1126/science.aad2087.

58. Wolfson, R.L., Chantranupong, L., Saxton, R.A., Shen, K., Scaria, S.M., Cantor, J.R., and Sabatini, D.M. (2016). Sestrin2 is a leucine sensor for the mTORC1 pathway. Science *351*, 43–48. 10.1126/science.aab2674.

59. Chantranupong, L., Scaria, S.M., Saxton, R.A., Gygi, M.P., Shen, K., Wyant, G.A., Wang, T., Harper, J.W., Gygi, S.P., and Sabatini, D.M. (2016). The CASTOR Proteins Are Arginine Sensors for the mTORC1 Pathway. Cell *165*, 153–164. 10.1016/j.cell.2016.02.035.

60. Saxton, R.A., Chantranupong, L., Knockenhauer, K.E., Schwartz, T.U., and Sabatini, D.M. (2016). Mechanism of arginine sensing by CASTOR1 upstream of mTORC1. Nature *536*, 229–233. 10.1038/nature19079.

61. Gu, X., Orozco, J.M., Saxton, R.A., Condon, K.J., Liu, G.Y., Krawczyk, P.A., Scaria, S.M., Harper, J.W., Gygi, S.P., and Sabatini, D.M. (2017). SAMTOR is an *S*-adenosylmethionine sensor for the mTORC1 pathway. Science *358*, 813–818. 10.1126/science.aao3265.

62. Chen, J., Ou, Y., Luo, R., Wang, J., Wang, D., Guan, J., Li, Y., Xia, P., Chen, P.R., and Liu, Y. (2021). SAR1B senses leucine levels to regulate mTORC1 signalling. Nature *596*, 281–284. 10.1038/s41586-021-03768-w.

63. Bonfils, G., Jaquenoud, M., Bontron, S., Ostrowicz, C., Ungermann, C., and De Virgilio, C. (2012). Leucyl-tRNA Synthetase Controls TORC1 via the EGO Complex. Mol. Cell *46*, 105–110. 10.1016/j.molcel.2012.02.009.

64. Sutter, B.M., Wu, X., Laxman, S., and Tu, B.P. (2013). Methionine Inhibits Autophagy and Promotes Growth by Inducing the SAM-Responsive Methylation of PP2A. Cell *154*, 403–415. 10.1016/j.cell.2013.06.041.

65. Tanigawa, M., Yamamoto, K., Nagatoishi, S., Nagata, K., Noshiro, D., Noda, N.N., Tsumoto, K., and Maeda, T. (2021). A glutamine sensor that directly activates TORC1. Commun. Biol. *4*, 1093. 10.1038/s42003-021-02625-w.

66. Chantranupong, L., Wolfson, R.L., and Sabatini, D.M. (2015). Nutrient-sensing mechanisms across evolution. Cell *161*, 67–83. 10.1016/j.cell.2015.02.041.

67. Jin, N., Mao, K., Jin, Y., Tevzadze, G., Kauffman, E.J., Park, S., Bridges, D., Loewith, R., Saltiel, A.R., Klionsky, D.J., et al. (2014). Roles for PI(3,5)P_2 in nutrient sensing through TORC1. Mol. Biol. Cell *25*, 1171–1185. 10.1091/mbc.e14-01-0021.

68. Kamada, Y., Yoshino, K., Kondo, C., Kawamata, T., Oshiro, N., Yonezawa, K., and Ohsumi, Y. (2010). Tor directly controls the Atg1 Kinase complex to regulate autophagy. Mol. Cell. Biol. *30*, 1049–1058. 10.1128/MCB.01344-09.

69. Suzuki, H., Osawa, T., Fujioka, Y., and Noda, N.N. (2017). Structural biology of the core autophagy machinery. Curr. Opin. Struct. Biol. *43*, 10–17. 10.1016/j.sbi.2016.09.010.

70. Suzuki, K., and Ohsumi, Y. (2010). Current knowledge of the pre-autophagosomal structure (PAS). FEBS Lett *584*, 1280–1286. 10.1016/j.febslet.2010.02.001.

71. Fujioka, Y., Alam, J.Md., Noshiro, D., Mouri, K., Ando, T., Okada, Y., May, A.I., Knorr, R.L., Suzuki, K., Ohsumi, Y., et al. (2020). Phase separation organizes the site of autophagosome formation. Nature *578*, 301–305. 10.1038/s41586-020-1977-6.

72. Kira, S., Kumano, Y., Ukai, H., Takeda, E., Matsuura, A., and Noda, T. (2016). Dynamic relocation of the TORC1–Gtr1/2–Ego1/2/3 complex is regulated by Gtr1 and Gtr2. Mol. Biol. Cell *27*, 382–396. 10.1091/mbc.e15-07-0470.

73. Wolfson, R.L., Chantranupong, L., Saxton, R.A., Shen, K., Scaria, S.M., Cantor, J.R., and Sabatini, D.M. (2016). Sestrin2 is a leucine sensor for the mTORC1 pathway. Science *351*, 43–48. 10.1126/science.aab2674.

74. Kim, A., and Cunningham, K.W. (2015). A LAPF/phafin1-like protein regulates TORC1 and lysosomal membrane permeabilization in response to endoplasmic reticulum membrane stress. Mol. Biol. Cell *26*, 4631–4645. 10.1091/mbc.E15-08-0581.

75. Hatakeyama, R. (2021). Pib2 as an Emerging Master Regulator of Yeast TORC1. Biomolecules *11*, 1489. 10.3390/biom11101489.

76. Mudholkar, K., Fitzke, E., Prinz, C., Mayer, M.P., and Rospert, S. (2017). The

Hsp70 homolog Ssb affects ribosome biogenesis via the TORC1-Sch9 signaling pathway. Nat. Commun. *8*, 937. 10.1038/s41467-017-00635-z.

77. Mülleder, M., Capuano, F., Pir, P., Christen, S., Sauer, U., Oliver, S.G., and Ralser, M. (2012). A prototrophic deletion mutant collection for yeast metabolomics and systems biology. Nat. Biotechnol. *30*, 1176–1178. 10.1038/nbt.2442.

78. Kira, S., Noguchi, M., Araki, Y., Oikawa, Y., Yoshimori, T., Miyahara, A., and Noda, T. (2021). Vacuolar protein Tag1 and Atg1–Atg13 regulate autophagy termination during persistent starvation in *S. cerevisiae*. J. Cell Sci. *134*, jcs253682. 10.1242/jcs.253682.

79. Kotani, T., Kirisako, H., Koizumi, M., Ohsumi, Y., and Nakatogawa, H. (2018). The Atg2-Atg18 complex tethers pre-autophagosomal membranes to the endoplasmic reticulum for autophagosome formation. Proc. Natl. Acad. Sci. *115*, 10363–10368. 10.1073/pnas.1806727115.

80. Merhi, A., and André, B. (2012). Internal amino acids promote Gap1 permease ubiquitylation via TORC1/Npr1/14-3-3-dependent control of the Bul arrestin-like adaptors. Mol. Cell. Biol. *32*, 4510–4522. 10.1128/MCB.00463-12.

81. Bianchi, F., Van'T Klooster, J.S., Ruiz, S.J., and Poolman, B. (2019). Regulation of Amino Acid Transport in Saccharomyces cerevisiae. Microbiol. Mol. Biol. Rev. *83*, e00024-19. 10.1128/MMBR.00024-19.

82. Kaur, J., and Bachhawat, A.K. (2007). Yct1p, a novel, high-affinity, cysteine-specific transporter from the yeast Saccharomyces cerevisiae. Genetics *176*, 877–

890. 10.1534/genetics.107.070342.

83. Düring-Olsen, L., Regenberg, B., Gjermansen, C., Kielland-Brandt, M.C., and Hansen, J. (1999). Cysteine uptake by Saccharomyces cerevisiae is accomplished by multiple permeases. Curr. Genet. *35*, 609–617. 10.1007/s002940050459.

84. Wu AL, M.-R.W. (1994). GSH1, which encodes gamma-glutamylcysteine synthetase, is a target gene for yAP-1 transcriptional regulation. Mol. Cell. Biol. *14*, 5832–5839. 10.1128/mcb.14.9.5832-5839.1994.

85. Kitamoto, K., Yoshizawa, K., Ohsumi, Y., and Anraku, Y. (1988). Dynamic aspects of vacuolar and cytosolic amino acid pools of Saccharomyces cerevisiae. J. Bacteriol. *170*, 2683–2686. 10.1128/jb.170.6.2683-2686.1988.

86. Kitajima, T., Jigami, Y., and Chiba, Y. (2012). Cytotoxic Mechanism of Selenomethionine in Yeast. J. Biol. Chem. *287*, 10032–10038. 10.1074/jbc.M111.324244.

87. Paul, B.D., Sbodio, J.I., and Snyder, S.H. (2018). Cysteine Metabolism in Neuronal Redox Homeostasis. Trends Pharmacol. Sci. *39*, 513–524. 10.1016/j.tips.2018.02.007.

88. Yin, J., Ren, W., Yang, G., Duan, J., Huang, X., Fang, R., Li, C., Li, T., Yin, Y., Hou, Y., et al. (2016). L-Cysteine metabolism and its nutritional implications. Mol. Nutr. Food Res. *60*, 134–146. 10.1002/mnfr.201500031.

89. Thomas, D., and Surdin-Kerjan, Y. (1997). Metabolism of sulfur amino acids in Saccharomyces cerevisiae. Microbiol. Mol. Biol. Rev. *61*, 503–532.

10.1128/mmbr.61.4.503-532.1997.

90. Varlakhanova, N.V., Mihalevic, M., Bernstein, K.A., and Ford, M.G.J. (2017). Pib2 and EGO Complex are both required for activation of TORC1. J. Cell Sci., jcs.207910. 10.1242/jcs.207910.

91. Kawano-Kawada, M., Kakinuma, Y., and Sekito, T. (2018). Transport of Amino Acids across the Vacuolar Membrane of Yeast: Its Mechanism and Physiological Role. Biol. Pharm. Bull. *41*, 1496–1501. 10.1248/bpb.b18-00165.

92. Stracka, D., Jozefczuk, S., Rudroff, F., Sauer, U., and Hall, M.N. (2014). Nitrogen source activates TOR (target of rapamycin) complex 1 via glutamine and independently of Gtr/Rag proteins. J. Biol. Chem. *289*, 25010–25020. 10.1074/jbc.M114.574335.

93. Dokládal, L., Stumpe, M., Hu, Z., Jaquenoud, M., Dengjel, J., and De Virgilio, C. (2021). Phosphoproteomic responses of TORC1 target kinases reveal discrete and convergent mechanisms that orchestrate the quiescence program in yeast. Cell Rep. *37*, 110149. 10.1016/j.celrep.2021.110149.

94. Albers, E., Laizé, V., Blomberg, A., Hohmann, S., and Gustafsson, L. (2003). Ser3p (Yer081wp) and Ser33p (Yil074cp) Are Phosphoglycerate Dehydrogenases in Saccharomyces cerevisiae. J. Biol. Chem. *278*, 10264–10272. 10.1074/jbc.M211692200.

95. Napolitano, G., Di Malta, C., Esposito, A., De Araujo, M.E.G., Pece, S., Bertalot, G., Matarese, M., Benedetti, V., Zampelli, A., Stasyk, T., et al. (2020). A substrate-

specific mTORC1 pathway underlies Birt–Hogg–Dubé syndrome. Nature *585*, 597–602. 10.1038/s41586-020-2444-0.

96. Morozumi, Y., Hishinuma, A., Furusawa, S., Sofyantoro, F., Tatebe, H., and Shiozaki, K. (2021). Fission yeast TOR complex 1 phosphorylates Psk1 through an evolutionarily conserved interaction mediated by the TOS motif. J. Cell Sci. *134*, jcs258865. 10.1242/jcs.258865.

97. Fan, S.-J., Snell, C., Turley, H., Li, J.-L., McCormick, R., Perera, S.M.W., Heublein, S., Kazi, S., Azad, A., Wilson, C., et al. (2016). PAT4 levels control amino-acid sensitivity of rapamycin-resistant mTORC1 from the Golgi and affect clinical outcome in colorectal cancer. Oncogene *35*, 3004–3015. 10.1038/onc.2015.363.

98. Hatakeyama, R., Péli-Gulli, M.-P., Hu, Z., Jaquenoud, M., Garcia Osuna, G.M., Sardu, A., Dengjel, J., and De Virgilio, C. (2019). Spatially Distinct Pools of TORC1 Balance Protein Homeostasis. Mol. Cell *73*, 325-338.e8. 10.1016/j.molcel.2018.10.040.

99. Meng, D., Yang, Q., Wang, H., Melick, C.H., Navlani, R., Frank, A.R., and Jewell, J.L. (2020). Glutamine and asparagine activate mTORC1 independently of Rag GTPases. J. Biol. Chem. *295*, 2890–2899. 10.1074/jbc.AC119.011578.

100. Baker Brachmann, C., Davies, A., Cost, G.J., Caputo, E., Li, J., Hieter, P., and Boeke, J.D. (1998). Designer deletion strains derived fromSaccharomyces cerevisiae S288C: A useful set of strains and plasmids for PCR-mediated gene disruption and

other applications. Yeast *14*, 115–132. 10.1002/(SICI)1097-0061(19980130)14:2<115::AID-YEA204>3.0.CO;2-2.

101. Sikorski, R.S., and Hieter, P. (1989). A System of Shuttle Vectors and Yeast Host Strains Designed for Efficient Manipulation of DNA in Saccharomyces ceratisiae. Genetics *122*, 19–27. 10.1093/genetics/122.1.19.

102. Waterhouse, A.M., Procter, J.B., Martin, D.M.A., Clamp, M., and Barton, G.J. (2009). Jalview Version 2—a multiple sequence alignment editor and analysis workbench. Bioinformatics *25*, 1189–1191. 10.1093/bioinformatics/btp033.

103. Janke, C., Magiera, M.M., Rathfelder, N., Taxis, C., Reber, S., Maekawa, H., Moreno-Borchart, A., Doenges, G., Schwob, E., Schiebel, E., et al. (2004). A versatile toolbox for PCR-based tagging of yeast genes: new fluorescent proteins, more markers and promoter substitution cassettes. Yeast *21*, 947–962. 10.1002/yea.1142.

104. Storici, F., and Resnick, M.A. (2006). The Delitto Perfetto Approach to In Vivo Site-Directed Mutagenesis and Chromosome Rearrangements with Synthetic Oligonucleotides in Yeast. In Methods in Enzymology (Elsevier), pp. 329–345. 10.1016/S0076-6879(05)09019-1.

105. Cools, M., Rompf, M., Mayer, A., and André, B. (2019). Measuring the Activity of Plasma Membrane and Vacuolar Transporters in Yeast. In Yeast Systems Biology Methods in Molecular Biology., S. G. Oliver and J. I. Castrillo, eds. (Springer New York), pp. 247–261. 10.1007/978-1-4939-9736-7_15.

106. Ishihama, Y., Oda, Y., Tabata, T., Sato, T., Nagasu, T., Rappsilber, J., and Mann, M. (2005). Exponentially Modified Protein Abundance Index (emPAI) for Estimation of Absolute Protein Amount in Proteomics by the Number of Sequenced Peptides per Protein. Mol. Cell. Proteomics *4*, 1265–1272. 10.1074/mcp.M500061-MCP200.

Acknowledgements

First, I would like to express my deepest gratitude to my supervisor, Prof. Takeshi Noda, for his continuous support, insightful guidance, and constructive feedback, throughout my research journey. I would like to express my deep gratitude to assistant professor Dr. Araki for his invaluable guidance and insightful discussion in this study. I am thankful to all members of Noda-Lab for valuable discussion.

I would like to thank for Prof. Takayuki Sekito and Prof. Nobuo Noda for their scientific discussions.

My heartfelt thanks go to my parents, for their unwavering love, support, and encouragement throughout my academic journey. I am immensely grateful to my spouse for her endless support, patience, and belief, and for always standing by my side, providing unwavering support in both the good times and the challenging moments.

Finally, I want to express my gratitude to everyone who took the time to read this thesis and provide me with valuable suggestions that will help me in my future studies.

Achievements

Publications

First author publication:

[1]．Qingzhong Zeng, Yasuhiro Araki, Takeshi Noda. Pib2 is a cysteine sensor involved in TORC1 activation. 投稿中.

[2]. Qingzhong Zeng, Yasuhiro Araki, Takeshi Noda. TORC1 represses SER3 expression by inducing lncRNA SRG1 transcriptional interference. 投稿準備中

[3]. Zhang, H.-T., **Zeng, Q**., Wu, B., Lu, J., Tong, K.-L., Lin, J., Liu, Q.-Y., Xu, L., Yang, J., Liu, X., et al. (2021). TRIM21-regulated Annexin A2 plasma membrane trafficking facilitates osteosarcoma cell differentiation through the TFEB-mediated autophagy. Cell Death Dis. 12, 21. 10.1038/s41419-020-03364-2. (Co-first author)

[4]. **Zeng, Q.**, Liu, W.T., Lu, J.L., Liu, X.H., Zhang, Y.F., Liu, L.X., and Gao, X.J. (2018). YWHAZ Binds to TRIM21 but Is Not Involved in TRIM21-stimulated Osteosarcoma Cell Proliferation. Biomed. Environ. Sci. BES 31, 186–196. 10.3967/bes2018.024.

Co-author publication:

[1]. Xu, G.-S., Lin, Y.-N., **Zeng, Q.**, Li, Z.-P., Xiao, T., Ye, Y.-S., Li, Z.-Y., and Gao, X. HSP90-regulated CHIP/TRIM21/p21 Axis Involves in the Senescence of Osteosarcoma Cells. Protein Pept. Lett. 30, 1–7.

[2]. Si, H.W., Mei, X.F., **Zeng, Q.**, Hui, L.X., Juan, G.X., and Xia, L.L. (2017). ERK1/2-mediated Cytoplasmic Accumulation of hnRNPK Antagonizes TRAIL-induced Apoptosis through Upregulation of XIAP in H1299 Cells. Biomed. Environ. Sci. 30, 473–481. 10.3967/bes2017.063.

[3]. Gao, X., Xu, F., Zhang, H.-T., Chen, M., Huang, W., Zhang, Q., **Zeng, Q.**, and Liu, L. (2016). PKCα–GSK3β–NF-κB signaling pathway and the possible involvement of TRIM21 in TRAIL-induced apoptosis. Biochem. Cell Biol. 94, 256–264. 10.1139/bcb-2016-0009.

[4]. Huang CQ, Li W, Wu B, Chen WM, Chen LH, Mo GW, Zhang QF, Gong L, Li J, Zhang HC, Zhu HM, **Zeng Q**. (2016). Pheretima aspergillum decoction suppresses inflammation and relieves asthma in a mouse model of bronchial asthma by NF-κB inhibition. J. Ethnopharmacol. 189, 22–30. 10.1016/j.jep.2016.05.028.

Conference Presentation

Qingzhong Zeng、荒木保弘、野田健司. 二つの TORC1 活性化経路の上流に位置するアミノ酸の同定. 第 11 回 TOR 研究会. (2021/7/15-16)

Qingzhong Zeng、荒木保弘、野田健司. オートファジーを抑制する TORC1 の活性化経路の上流に位置するアミノ酸の同定. 「マルチモードオートファジー」第 3 回班会議・第 14 回オートファジー研究会. (2021/10/24-27)

Qingzhong Zeng, Yasuhiro Araki, Takeshi Noda. TORC1 senses amino acids through distinct upstream pathways to inhibit autophagy. The 10th International Symposium on Autophagy. (2022/10/23-27)

Qingzhong Zeng, Yasuhiro Araki, Takeshi Noda. Cysteine-activated TORC1 is dependent on the Pib2 pathway in Saccharomyces cerevisiae. 第 12 回 TOR 研究会. (2022/10/29-30)

Qingzhong Zeng, Yasuhiro Araki, Takeshi Noda. Cysteine-activated TORC1 is dependent on the Pib2 pathway. The 45th Annual Meeting of the Molecular Biology Society of Japan. (2022/11/30-12/2)